Since January 2020 Elsevier has created a COVID-19 resource centre with free information in English and Mandarin on the novel coronavirus COVID-19. The COVID-19 resource centre is hosted on Elsevier Connect, the company's public news and information website.

Biomedicine & Pharmacotherapy 132 (2020) 110902

Contents lists available at ScienceDirect

Biomedicine & Pharmacotherapy

journal homepage: www.elsevier.com/locate/biopha

Review

Aptamers used for biosensors and targeted therapy

Yi Ning, Jue Hu, Fangguo Lu *

Department of Microbiology, The Medicine School of Hunan University of Chinese Medicine, Changsha, Hunan, 410208, PR China

ARTICLE INFO

Keywords:
Aptamer
SELEX
Aptasensor
Targeted drug delivery
Nucleic acid therapeutics

ABSTRACT

Aptamers are single-stranded nucleic acid sequences that can bind to target molecules with high selectivity and affinity. Most aptamers are screened in vitro by a combinatorial biology technique called systematic evolution of ligands by exponential enrichment (SELEX). Since aptamers were discovered in the 1990s, they have attracted considerable attention and have been widely used in many fields owing to their unique advantages. In this review, we present an overview of the advancements made in aptamers used for biosensors and targeted therapy. For the former, we will discuss multiple aptamer-based biosensors with different principles detected by various signaling methods. For the latter, we will focus on aptamer-based targeted therapy using aptamers as both biotechnological tools for targeted drug delivery and as targeted therapeutic agents. Finally, challenges and new perspectives associated with these two regions were further discussed. We hope that this review will help researchers interested in aptamer-related biosensing and targeted therapy research.

1. Introduction

Aptamers, first raised by two research groups independently in 1990 [1,2], are single-stranded DNA (ssDNA) or RNA sequences obtained through systematic evolution of ligands by exponential enrichment (SELEX) that can fold into secondary and three-dimensional shapes, enabling them to recognize various target molecules with high specificity and affinity, including proteins [3,4], small molecules [5,6], metal ions [7,8], bacterial cells [9,10], viruses [11,12], cancer cells [13,14], and even tissues [15]. Owing to the high binding affinity and selectivity of an aptamer to its target, it is also termed a chemical antibody with dissociation constants (K_d) in the pico to nanomolar range [16–18]. Compared to antibodies, aptamers possess the following merits [19]. First, aptamers can be obtained via an in vitro process without the need for complex cell or animal experiments. This allows them to bind ligands that are not recognized by the antibody, such as inorganic ions and small molecules [20]. Second, aptamers can be massively amplified by polymerase chain reaction (PCR) in a short time, which is more time efficient and cheaper than the preparation of antibodies [21]. Third, aptamers are easily modified with functional moieties (e.g., fluorophores, quenchers, and nanomaterials) via physical adsorption or chemical coupling because of their simple chemical structures [22–24]. Fourth, aptamers are safer in vivo than antibodies owing to their non-immunogenic characteristics [25]. Finally, aptamers are more stable under harsh conditions than antibodies [26].

Because of these predominant advantages, aptamers are considered potential alternatives to antibodies in many fields. Up to now, the applications of aptamers include diagnostics [27,28], therapeutics [29,30], cell imaging [31,32], drug delivery [33,34], selective chromatography [35,36], biosensing [37–40], and biomarker discovery [41,42], to name a few (some aptamer-based applications are shown in Fig. 1). Numerous reviews on aptamers have been published in recent years with different emphases [43–45]. In this review, we provide an overview of aptamer-based biosensors and targeted therapy. Additionally, we also attempt to discuss the challenges faced in these two areas with the purpose of paving the way for the better use of aptamers in bioassays and clinical treatment.

2. Aptamer selection

2.1. General

Aptamers are developed against any desired molecule using SELEX. Fig. 2 displays a typical SELEX process. Generally, the process of SELEX includes three steps, which are repeated to generate aptamers that fit their targets. In the first step (library generation), a random library is artificially designed and synthesized by a combinatorial chemical synthesis technique. These oligonucleotides consist of 20–40 bases in the middle, flanked by up- and downstream primer binding sites at each end, which enabled the library to contain 10^{12}–10^{15} ssDNA or RNA

* Corresponding author.
E-mail address: lufgny@163.com (F. Lu).

https://doi.org/10.1016/j.biopha.2020.110902
Received 18 August 2020; Received in revised form 12 October 2020; Accepted 14 October 2020
Available online 20 October 2020

sequences [46]. In the second step (selection), the target molecule is first incubated with the library for several minutes in binding buffer. In theory, the aptamers will specifically bind to their targets, and other non-specific sequences will stay in the binding buffer. The aptamer-target complexes were collected and washed several times with washing buffer. Then, the aptamers were separated from the aptamer-target complex by treating with elution buffer. In this step, counter-selection is usually implemented to eliminate those that do not bind to the target of interest. During counter-selection, the target is replaced by analogs for one selection round, and the nucleic-acid sequences that bound to the analogs were excluded from the library prior to the next round of selection with the target. In addition, the selection parameters will become increasingly stringent with the increase in the number of selection rounds. These measures greatly increase the pressure in the screening process, making the specific aptamers against the target continuously enriched [47,48]. In the third step (amplification), the sequences eluted from the target are amplified by employing PCR for DNA and reverse transcriptase (RT)-PCR for RNA to produce a sub-library for the next round of selection. These three steps consist of one cycle of SELEX. When the affinities of the sequences bound to the target are saturated, the sequences from the last round are sent to the clone and sequence, followed by the identification of aptamer sequences that bind the target with high sensitivity and specificity.

2.2. Nitrocellulose membrane filtration-based SELEX

Nitrocellulose membrane filtration is the first partitioning technique to retain the complexes and remove the unbound oligonucleotide sequences based on the size of molecules. Hence, it is effective for the separation of macromolecules. The nitrocellulose membrane is a popular binding matrix for western blotting because of its high affinity to proteins. Many pores of micron size on the surface of nitrocellulose membranes allow DNA or RNA oligonucleotides to pass through and the protein to be trapped on the membrane. After incubating the target with the library, the mixture was transferred onto a nitrocellulose membrane. The aptamer-target complex retained by the nitrocellulose membrane was washed thoroughly, and the bound aptamers were eluted and amplified by PCR or RT-PCR for the next round of reaction. Several RNA aptamers, including T4 DNA polymerase [2], reverse transcriptase (HIV-1) [49], human IgE [50], vascular endothelial growth factor (VEGF) [51], mouse prion protein [52], and ricin A chain [53], have been obtained by using this filter binding process, demonstrating the suitability of nitrocellulose membranes for efficiently isolating RNA from its protein complex. However, nitrocellulose membranes have some shortcomings, such as low separation efficiency and showing no effect toward small molecules, ions, and peptides. Moreover, at least 12 selection rounds are needed [54,55].

2.3. Affinity chromatography and magnetic bead-based SELEX

To improve the separation efficiency, affinity chromatography and magnetic bead-based SELEX were developed. Affinity chromatography, an approach with a highly specific affinity, can separate the targets from a complex mixture. It is mainly employed to purify recombinant proteins based on the specific recognition between the receptor and the ligand. Agarose beads packed onto a column are generally used as the stationary phase. After several rounds of washing and elution processes, only the oligonucleotides in the library with high affinity to the target can be captured, and other unbound oligonucleotides will be eliminated in the rounds of selection (Fig. 3A). Various tags are used for the immobilization of proteins, such as glutathione S-transferase (GST) and the His-tag. Additionally, covalent coupling is utilized for fixing small organic molecules onto beads, such as the formation of amide bonds via N-(3-dimethylaminopropyl)-N′-ethylcarbodiimide hydrochloride and N-hydroxysuccinimide (EDC/NHS) catalysis [56]. Hence, this method can be implemented for the selection of not only aptamers of proteins, but also small organic molecules [57,58]. Several aptamers screened by affinity chromatography-based SELEX have been reported so far, including aptamers against lysozymes [59], biotoxins [60], prions [61], and HSV-1 US11 [62]. Magnetic beads are also used for the immobilization of the target through a physical interaction or chemical reaction between a specific tag and its ligand on the beads. After the target protein was immobilized on magnetic beads, an oligonucleotide library was added, followed by isolation of the aptamer-target complex from the

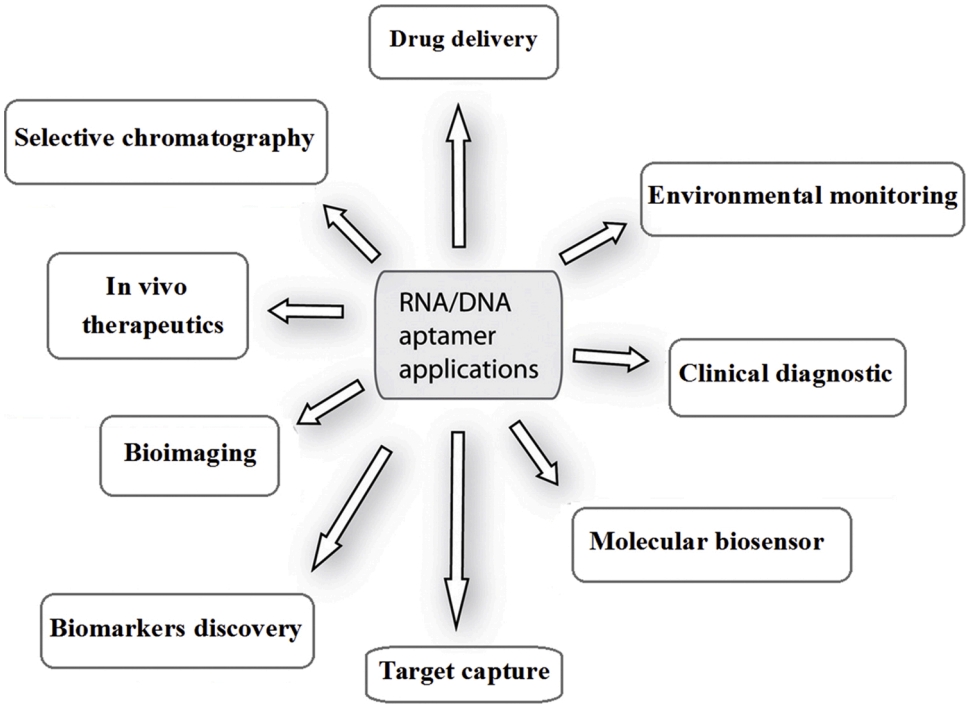

Fig. 1. Various application fields of aptamers.

unbound oligonucleotides using a magnet (Fig. 3B) [63]. In this method, magnetic beads are regarded as a particularly effective tool for the separation of aptamer-target complexes with a magnetic separator, which makes it widely used for several aptamer selections, such as streptavidin [63], ibuprofen [64], polychlorinated biphenyls [65], and *Escherichia coli* K88 [66]. The above two methods require only very small amounts of target and allows easy operation, but cannot be executed if the target lacks the affinity tag or functional group required for linking to the beads. Moreover, the beads probably close the functional site of the target that is suitable for aptamer binding. In this case, the selected aptamer did not work in the analysis of actual samples.

2.4. Capillary electrophoresis and microfluidic-based SELEX

With the development of equipment, capillary electrophoresis SELEX (CE-SELEX) and microfluidic SELEX (M-SELEX) have been reported. CE-SELEX is superior to many other analytical separation methods in terms of speed, resolution, capacity, and minimal sample dilution. It can be performed without immobilizing the target on a solid matrix, and usually requires fewer selection cycles for the identification of aptamers. In addition to maintaining the affinity between the aptamer and its target, this method can reduce the number of rounds of aptamer selection from 15 in traditional SELEX to four in CE-SELEX [67–69]. In this method, separation of the target bound oligonucleotides from unbound oligonucleotides in the electric field depends on the difference in electrophoretic mobility caused by different charges, frictional forces, and hydrodynamic radii (Fig. 4A) [70]. In the capillary, an aptamer can be obtained by the migration speeds of the mixture of target, ligand, or target-ligand complexes. To date, aptamers against alpha-fetoprotein [71], neuropeptide Y [72], human IgE [73], and ovarian cancer biomarker HE4 [74] have been selected using CE-SELEX. A modified CE-based selection method, called non-SELEX, has been introduced to select an aptamer without needing PCR amplification of the oligonucleotide sequences. In this strategy, the oligonucleotide–target complex is separated from unbound oligonucleotides by a highly efficient affinity method named non-equilibrium capillary electrophoresis of equilibrium mixtures (NECEEM), and the selection process can be completed within 1 h [75]. However, the volume of the library injected into the capillary is very small, which limits the number of sequences (~10^{12} sequences) for target binding [76]. To address this shortcoming, micro free flow electrophoresis (μFFE) was developed [77]. In this improved method, the size of the sequences in the initial pool can peak at ~10^{14} sequences, which is about 300 times that in CE-SELEX. However, owing to the preparation requirements of special μFFE instruments, the process takes a long time. Moreover, only one aptamer can be achieved using this method. The microfluidic system is an automated and miniature platform that enables aptamer selection on a chip. In order to realize the selection process automatically, several modules, including micropumps, microvalves, a pressurized reagent reservoir manifold, reagent loading chambers, reagent-loaded micro--lines, temperature control modules, transportation units, waste chambers, and PCR chambers, are orderly integrated. Because this method is mainly processed on a chip, it is possible to implement repetitive rounds of extraction and amplification in a short time via this automatic device [78,79]. The microfluidic SELEX technique can be considerably improved by combining it with magnetic bead-based separation. In 2009, a rapid and automatic aptamer selection system, which integrates the magnetic bead-based SELEX process with microfluidics technology and a continuous-flow magnetic activated chip-based separation (CMACS) device, was designed (Fig. 4B) [80]. Using this approach, an enriched aptamer pool, which is specifically bound to recombinant botulinum neurotoxin type A, was obtained through only one round of selection. However, the magnetic beads in the microchannel might aggregate together in the process of selection, resulting in low purity and aptamer recovery. Additionally, microbubbles will be produced, which might lead to the flow streams being distorted. To overcome these

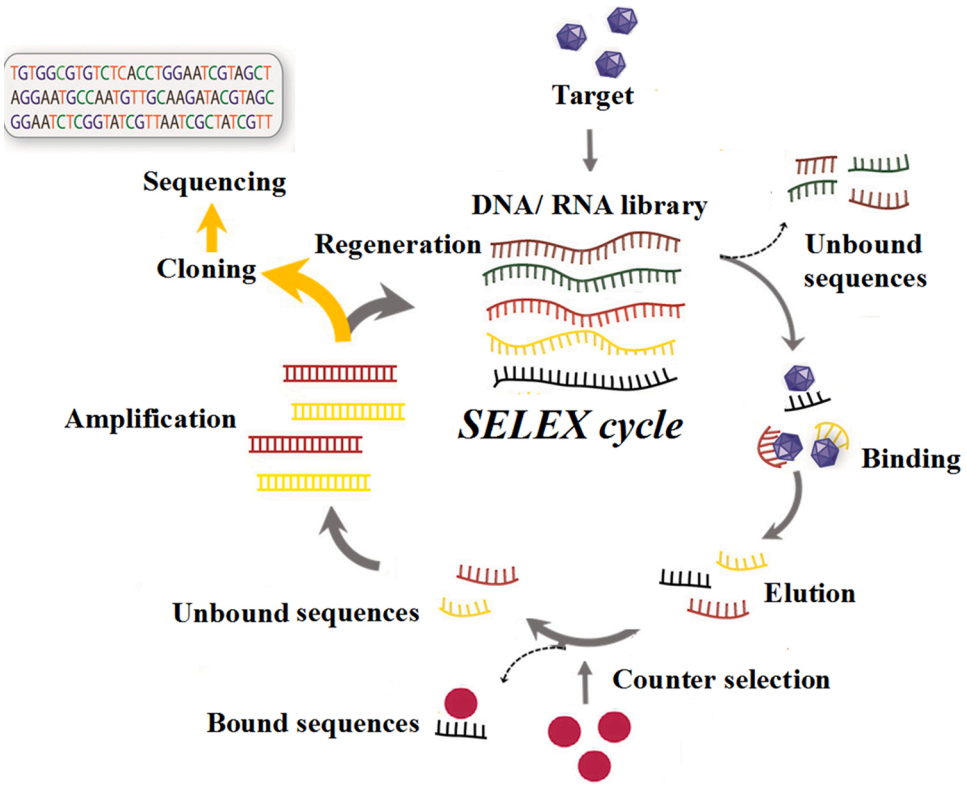

Fig. 2. Schematics of SELEX process. The DNA or RNA library are generated by combinatorial chemical synthesis. Identification of high affinity aptamers usually involves iterative cycles of aptamer selection. Each selection cycle includes ligand binding, partition, elution and amplification. After several selection rounds, cloning and sequencing steps are implemented followed by evaluation of target affinity of the enriched aptamers.

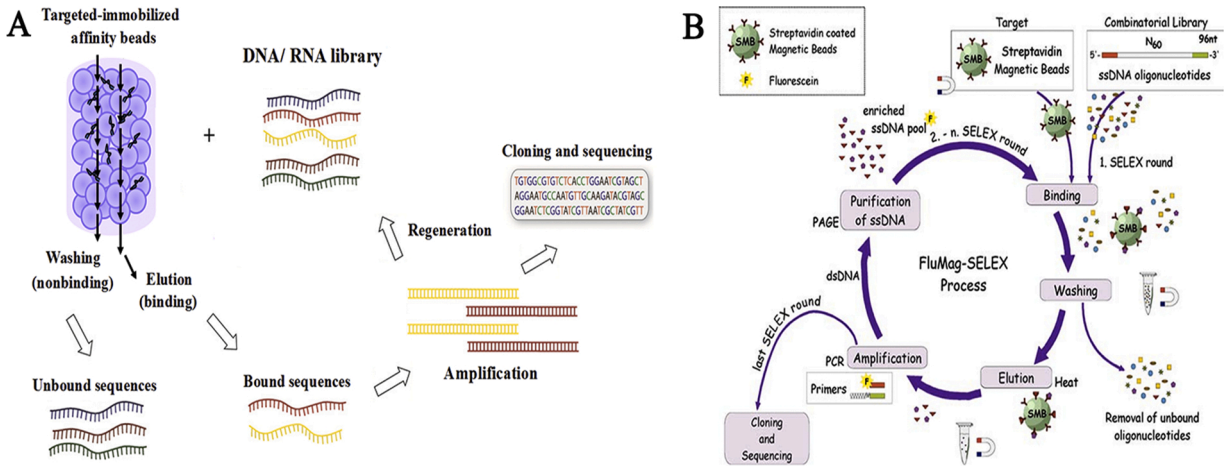

Fig. 3. Schematic illustration of affinity chromatography and magnetic bead-based SELEX. (A) A schematic illustration of the selection step from a library using an affinity column. Target is immobilized onto affinity beads, then the DNA/ RNA library is added. After several rounds selection, the oligonucleotides in the library that are captured by the target with high affinity are identified; (B) Schematic representation of the fluorescence-monitored SELEX (FluMag-SELEX) for selecting DNA aptamers for specific target molecules (here streptavidin) immobilized on magnetic beads. The initial ssDNA library was incubated with the target beads for binding. Unbound sequences were discarded and the bound sequences were eluted from the target beads by heat treatment. The bound sequences were amplified by PCR for the next SELEX round. The selected aptamers in the last round were sent to clone and sequence followed by affinity evaluation. Fig. 3B adapted from ref. [63].

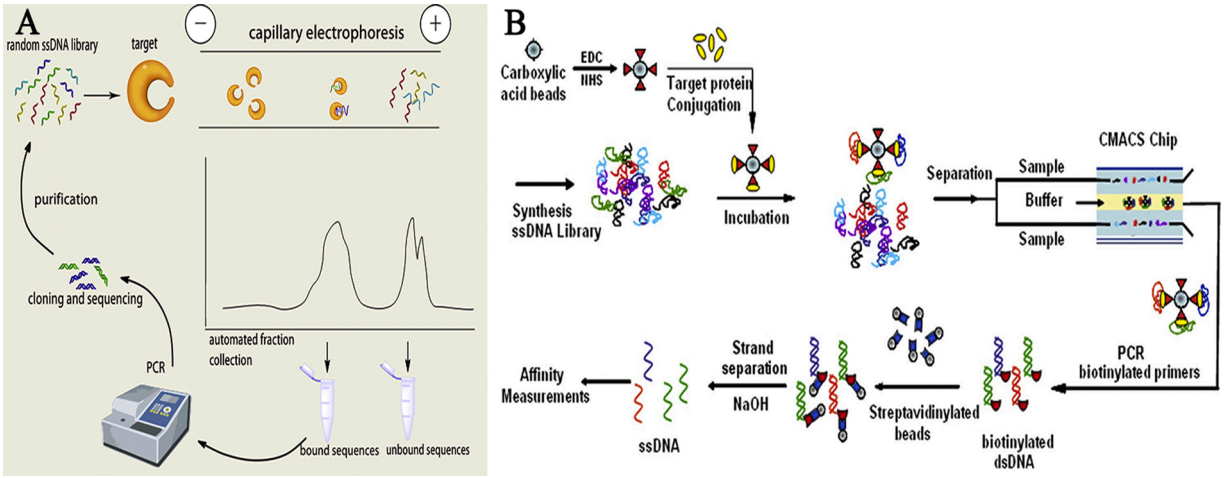

Fig. 4. Schematic illustration of capillary electrophoresis and microfluidic-based SELEX. (A) A schematic of the CE-SELEX strategy. A ssDNA pool is mixed with target. The mixture is injected into CE system for separation, and the peaks of aptamer-target complex and the unbound ssDNA are collected. The bound sequences are eluted for the next round of selection. Fig. 4A adapted from ref. [70]; (B) Flowchart for the M-SELEX process. A target protein is conjugated to magnetic beads via covalent coupling and then mix with ssDNA pool. Aptamers that bind to the target protein are isolated by employing the CMACS device. The bounded aptamers are amplified via PCR followed by treatment with sodium hydroxide for generating ssDNA. Fig. 4B adapted from ref. [80]. Copyright (2009) National Academy of Sciences.

disadvantages, using ferromagnetic materials to prepare the micro-channel can greatly improve M-SELEX. Using this method, an aptamer with a K_d value of 25 nM against streptavidin was obtained in only three rounds of selection [81]. Overall, M-SELEX is an effective method that can considerably enhance the efficiency of aptamer selection. However, it has its shortcomings, such as an unstable injection volume and the requirement of other nanomaterial modifications to enhance the hydrophilicity of micro-channels. Furthermore, each research group has to spend a large amount of time designing microfluidic devices owing to its non-commercial property.

2.5. Other method-based SELEX

Several methods, such as atomic force microscopy [82], high-throughput sequencing [83,84], graphene oxide (GO) [85,86], cross-linking by UV [87,88], flow cytometry [89,90], and surface plasmon resonance (SPR) [91,92], have been fabricated in connection with SELEX for aptamer selection. These methods not only enrich the selection measures, but also promote the efficiency of aptamer selection. Based on the above strategies, various aptamers have been selected and identified, which lay the foundation for the construction of aptamer-based biosensors for bioassays and targeted therapies for clinical treatment.

3. Aptamer-based biosensor

3.1. General

A typical biosensor consists of two basic components: a recognition element (antibody, biological tissue, antigen, nucleic acid, enzyme, etc.) and a signal transducer (fluorescent, electrochemical, colorimetric, chemiluminescent, etc.) [93,94]. Biosensors that are based on aptamers

as biorecognition elements are named aptasensors. Aptamers used in the field of biosensors make use of their high affinity and tunable properties, while their sensitivity is greatly influenced by the transducer. Until now, many papers concerning the preparation of aptamer-based biosensors have been published. These aptasensors were constructed using various methodologies, such as optical aptasensors (fluorescence-based optical aptasensors and colorimetric-based optical aptasensors), electrochemical aptasensors, chemiluminescent aptasensors, and surface-enhanced Raman scattering (SERS) aptasensors [95–99]. However, most of the principles of these aptasensors have some versatile or analogous elements. Among these design strategies, we will explore three general modes that have emerged most frequently in the literature: structure-switching mode, enzyme-assisted recycling mode, and split aptamer-based mode.

3.2. Structure-switching designs

The most common mode reported in previous studies is the structure-switching mode. In this mode, a quencher-labeled complementary DNA (cDNA) is often designed to bind a fluorophore-labeled aptamer. Initially, the fluorescence is quenched owing to the closeness of the fluorophore and quencher. When the target is added, the fluorophore-labeled aptamer specifically binds to the target, leading to the fluorescence enhancement (Fig. 5A) [100]. The fluorophore/quencher can also be replaced by other types of signal transduction, such as gold nanoparticles [101], carbon dots [102], quantum dots [103], or electrode surfaces [104]. Xiao et al. designed a redox probe-labeled, signal-off electrochemical aptasensor for thrombin analysis. Before adding the thrombin, methylene blue (MB) covalently labeled onto the aptamer could transfer electrons to the electrode surface because of the flexible conformation of the aptamer. After adding thrombin, a G-quaduplex structure was formed and the MB moiety was far away from the electrode surface, resulting in the electrochemical signal-off (Fig. 5B) [105]. The main disadvantage of this signal-off electrochemical method is that it easily produces a negative signal. To overcome this shortcoming, Zuo et al. designed a target-responsive and signal-on electrochemical aptamer switch (TREAS) for the reagentless detection of adenosine triphosphate (ATP) [106]. In this strategy, an anti-ATP aptamer dually labeled with 3′-SH and 5′-ferrocene that is hybridized to its cDNA is self-assembled on gold electrodes in duplex form. In the absence of the target, ferrocene could not exchange electrons with the gold electrodes because of the large distance between them, which leads to an eT OFF state. Upon the addition of the target, the aptamer-target tertiary structure was formed, which subsequently denatured the duplex and liberated the cDNA. As a result of this structural switch from the duplex to the tertiary structure, the ferrocene moiety was close to the electrode surface and produced apparent electrochemical signals (eT ON). Signal-on designs can generate positive signals, which obviously broaden their applications for many analyte assays. Colorimetric-based optical strategies based on gold nanoparticles were also developed to construct structure-switching aptasensors. Liu and Lu fabricated an adenosine-responsive aptamer-linked AuNP disassembly system. The system consisted of two kinds of DNA-functionalized AuNPs and linker DNA. The linker DNA contained an adenosine aptamer fragment and extension sequence. In the presence of adenosine, AuNPs were close to each other because of the bridging effect of the linker DNA, leading to the aggregation of AuNPs. Hence, the reaction solution displayed a purple color. In the presence of adenosine, the aptamer binds to adenosine and folds to the complex structure. The AuNPs were then released into the solution, changing the color from purple to red (Fig. 5C) [107]. Structure-switching designs were also employed for the detection of other targets, such as vitamin D3 [108], abscisic acid [109], cancer cells [110], interleukin-6 [111], and chloramphenicol [112]. These methods based on AuNPs are simple and cost-effective because the color change can be conveniently assayed by the naked eye. However, they may suffer from high background signals, which would affect the sensitivity of the aptasensors.

Some sensors designed as aptamer beacons were frequently constructed for analyzing many targets. The aptamer beacon (aptabeacon) has a hairpin-shaped structure, where its 5′ and 3′ ends are labeled with a fluorophore and quencher that forms a stem of the aptamer-predicted structure and the loop serving as a recognition element for the target. Without the target, the fluorescence is low because of the occurrence of fluorescence resonance energy transfer (FRET) between the fluorophore

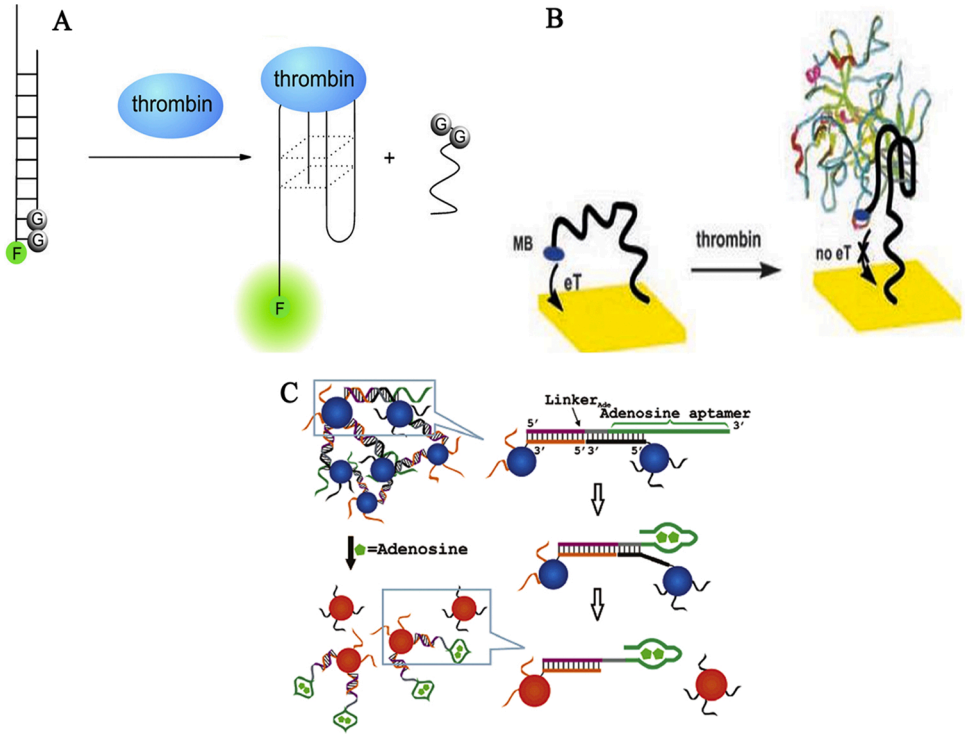

Fig. 5. Various signals generated by aptasensor based on structure-switching designs. (A) A schematic representation of the fluorescent aptasensor for thrombin assay. Thrombin-induced structure change of the aptamer from quenching-state into G-quartet structure could lead to fluorescence enhancement. Fig. 5A adapted from ref. [100]; (B) A schematic representation of the electrochemical aptasensor for thrombin assay. Before adding the thrombin, MB covalently labeled onto aptamer could transfer electron with the electrode surface due to the flexible conformation of the aptamer. Upon adding the thrombin A, G-quaduplex structure was formed and the MB moiety was far away from the electrode surface, resulting in the electrochemical signal-off. Fig. 5B adapted from ref. [105]; (C) A schematic representation of the colorimetric aptasensor for adenosine assay. Gold nanoparticles are functionalized with aptamer. Addition of the adenosine results in nanoparticles linking together and aggregating, thus causing the change in color. Fig. 5C adapted from ref. [107]. Copyright (2007) American Chemical Society.

and quencher. After introducing the target, the rigid structure of the beacon is destroyed, resulting in the restoration of the fluorescence due to the farawayness of the fluorophore and quencher [113,114]. Sanzani et al. developed an aptabeacon in which a DNA aptamer was used as a recognition probe in its molecular beacon form with a fluorescence (FAM)-quenching (BHQ1) pair at the stem ends for quantitative determination of ochratoxin A (OTA) in wine. In the absence of the target, the aptabeacon maintained its quenched stem-loop structure. In contrast, the conformation of the hairpin would be shifted, generating an apparent fluorescence signal due to the increased distance between FAM and BHQ1 (Fig. 6A) [115]. DNA intercalating dye that could be inserted into the stem of the beacon can also be used for this design. Chi et al. fabricated a quantum dot (QD)-aptamer (apt) beacon that acts by the folding-induced dissociation of a DNA intercalating dye (BOBO-3) for label-free thrombin detection. In this strategy, an antithrombin aptamer probe, which requires no fluorophore or quencher labels on its 5′ and 3′ sites, is covalently linked to Qdot 565 (peak emission at 565 nm). Then, BOBO-3 was intercalated into the double helix, and the QD-apt:B beacon was created. Before binding thrombin, the FRET-mediated emission of BOBO-3 could be measured when the QD was illuminated at 365 nm. After introducing thrombin, the stem-loop structure of the beacon changed to quadruplex, leading to the release of BOBO-3 from QD-apt. Hence, the FRET-mediated emission of BOBO-3 was terminated (Fig. 6B) [116]. The aptabeacon used for bioassays shows advantages in simplicity, directness, and rapidity. However, it cannot be used to detect non-specific ssDNA-binding proteins, and its conformation is greatly affected by some metal ions that will affect the fluorescence detection. Additionally, the enhancement of sensitivity is still a crucial issue for developing these techniques. With the development of micro-detection and spectrum technology, combined with the application of nucleases and inorganic nanoparticles in the design of molecular beacons, it is possible to improve the sensitivity of the detection methods using molecular beacons [117–119].

In addition to using cDNA to lock the initial aptamer conformation and designing the stem-loop aptabeacon, a nanomaterial, such as graphene oxide (GO), is intensively used as the a nanoscaffold to adsorb ssDNA probes. GO, a two-dimensional carbon material, has attracted considerable attention owing to its prominent physical, chemical, thermal, and mechanical properties [120,121]. GO that can be used to build aptasensors is based on these three main properties. First, GO has a large surface area for binding nucleic acids via π-stacking interactions or chemical modifications [122,123]; second, GO can act as a superb quencher through FRET experiments because of its broad absorption spectrum and high quenching efficiency [124,125]; finally, GO can protect nucleic acids that bind to its surface from being cleaved by nucleases in a biological environment [126,127]. Tan et al. designed aptasensor for the analysis of chloramphenicol (CAP), which is based on double signal amplification and GO as an efficient fluorescence quencher. In this method, a nucleic acid probe containing two FAM-labeled signal probes (SPs) and a capture probe (CP) was adsorbed onto the surface of GO via π-stacking interactions without the CAP. This adsorption results in the quenching of the fluorescence of the label. Upon addition of CAP, the fluorescence was restored because the aptamer/CAP complexes were formed, which led to the FAM being away from GO (Fig. 7A) [128]. Using a dye-labeled probe/GO quenching model, various targets, including IgE [129], aflatoxin B-1 [130], platelet-derived growth factor-BB (PDGF-BB) [131], and *Salmonella* [132], have been successfully detected. Ning et al. fabricated a label-free fluorescent aptasensor for the determination of ATP. This aptasensor was composed of unbound SYBR Green I, graphene oxide, and a label-free detection probe. In the absence of ATP, the probe was adsorbed on the GO surface and no fluorescence appeared. When ATP and cDNA were added, the probe was dissociated from GO, forming a DNA-SYBR Green I complex that generated obvious fluorescence. Compared to the first method, this approach does not involve labeling at the end of the probe, which is simple and cost-effective. In addition, false-positive signals can be avoided due to the high transfer efficiency between GO and the SYBR Green I-DNA duplex structure (Fig. 7B) [133]. Overall, the GO-based aptasensor has the merits of high sensitivity, quick response, good reproducibility, and stability, making it a promising candidate for environmental monitoring, medical diagnostics, and food safety assays.

3.3. Enzyme-assisted recycling design

Enzyme-assisted target recycling and signal amplification designs have attracted significant attention owing to their high sensitivity [134]. To date, different types of nucleases, such as polymerases [123,135], exonucleases [136,137], deoxyribonucleases [132,138], and endonucleases [139,140], have been frequently employed to construct aptasensors for many target assays. The different properties of these nucleases can trigger several rounds of target recycling by implementing their endonuclease reaction or polymerization reaction. Hence, only a small number of targets are needed to produce an apparent signal, which greatly enhances the sensitivity of the aptasensor.

3.3.1. Deoxyribonuclease I

Deoxyribonuclease I (DNase I) is a common endonuclease that can digest ssDNA and dsDNA randomly and simultaneously. Aptamer, an ssDNA that can form a special structure after binding to the target, can also be cleaved by DNase I, which leads to target recycling. Ning et al. developed an amplified aptamer-based sensor for assaying ATP based on DNase I and GO. They designed a DNA probe containing two partially complementary sequences that represented the CP and SP, respectively. In the absence of ATP, GO can strongly adsorb the DNA probe via π-stacking interactions, which results in the quenching of the fluorescent label and protects the probe from nuclease cleavage. Upon the addition of ATP, the probe dissociated from GO due to specific recognition between the aptamer and ATP, inducing an increase in the fluorescence intensity. Importantly, DNase I could degrade the aptamer, releasing

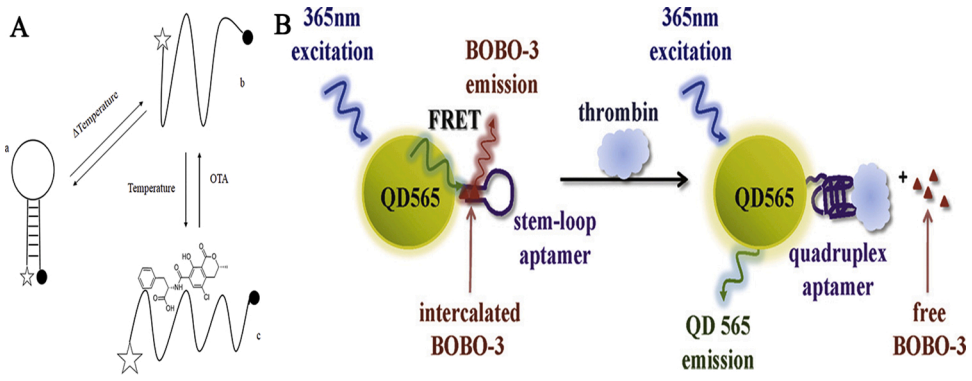

Fig. 6. Aptabeacon designed for bioassay based on structure-switching designs. (A) Schematic representation of dual labeled aptabeacon for OTA assay. Addition of the OTA results in the change of stem-loop conformation, causing the fluorescence enhancement. Fig. 6A adapted from ref. [115]; (B) Schematic representation of QD-apt:B beacon for label-free detection of thrombin. Thrombin binding triggers the conformational change of the aptamer on QD, causing the dissociation of the stained BOBO-3 from QD-apt. Thus, the quantity of thrombin can be measured by the decrease of QD FRET-mediated BOBO-3 emission. Fig. 6B adapted from ref. [116].

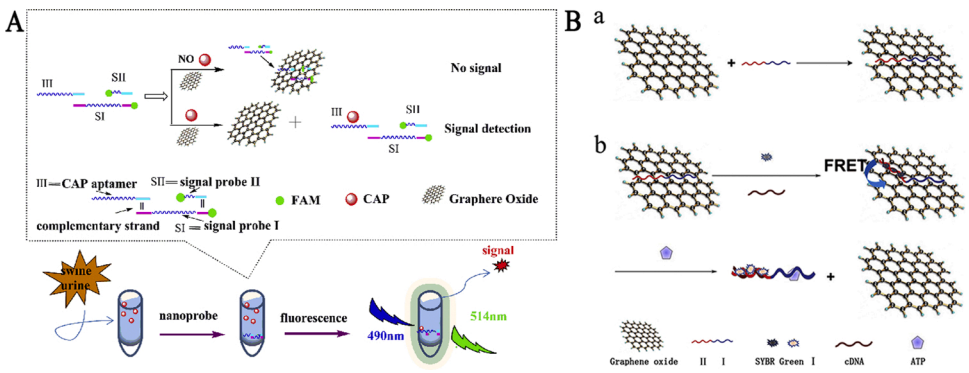

Fig. 7. GO-based aptasensor for bioassay based on structure-switching designs. (A) Scheme of the strategy for CAP determination based on GO fluorescent nanoprobe. Without CAP, the nanoprobe adsorbed onto GO, leading to the quenching of the FAM. Addition of the CAP leads to the restoration of fluorescence due to the removal of the probes from GO. Fig. 7A adapted from ref. [128]; (B) Schematic representation of the probe/GO platform for label-free detection of ATP. a) Without ATP, the probe adsorbed onto GO and the fluorescence of SG was quenched. b) On the contrary, ATP binding induced enhancement of fluorescence. Fig. 7B adapted from ref. [133].

ATP and FAM fluorophores simultaneously. The released target then bound to another aptamer, resulting in the accumulation of free FAM fluorophores (Fig. 8A) [141]. Using this approach, the limit of detection (LOD) of ATP could reach 0.2 nM. A similar DNase I-based amplification method was proposed by Lin et al. for assaying ATP using carbon nanoparticles instead of GO. The LOD of this sensing platform was also calculated as 0.2 nM [142]. Recently, nano-graphite (NG), similar to GO, is a prominent carbon nanomaterial that has attracted attention globally because of its unique physical and chemical properties compared to those of GO [143,144]. Because they have the same fluorescence quenching mechanism, NG can also be used for target analysis based on DNase I-based amplification. Wei et al. reported an aptamer/NG sensing system for Ag^+ detection. In the absence of Ag^+, the C-rich ssDNA labeled with a fluorescein (ROX) was adsorbed on NG via π-stacking interactions, and the fluorescence was quenched as a result of FRET between ROX and NG. Upon the addition of Ag^+, C-Ag^+-C coordination triggered the aptamer to form a hairpin structure, which led to the dissociation of the aptamer/Ag^+ complex from NG. Hence, this resulted in the enhancement of fluorescence. Additionally, DNase I-assisted digestion of the Ag^+-ssDNA complex occurred, releasing the target for binding to another ROX-labeled ssDNA. This process led to the recycling of Ag^+ and accumulation of free ROX fluorophores, which could improve the sensitivity toward Ag^+ (Fig. 8B) [145]. The LOD of this sensing system used for the Ag^+ assay was 0.3 nM, which was much lower than the standard for Ag^+ in drinking water recommended by the Environmental Protection Agency (EPA). Besides the detection of ATP and Ag^+, other targets, including mucin 1 protein (MUC1) [146], ochratoxin-A (OTA) [147], and *Salmonella enteritidis* [148], were also detected using DNase I-assisted target recycling and signal amplification designs.

3.3.2. *Klenow fragment (KF)*

The Klenow fragment (KF), a large fragment of DNA polymerase I, possesses 5′-to-3′ polymerase activity and 5′-to-3′ exonuclease (proofreading) activity, but lacks the 5′-to-3′ exonuclease activity of DNA polymerase I. This characteristic could induce the occurrence of a strand-displacement polymerization reaction (SDPR) for target recycling, generating many dsDNAs simultaneously. Lin et al. created an aptasensor for the rapid detection of enterotoxigenic *Escherichia coli* (ETEC) K88 based on KF-aided target recycling amplification and GO. In this strategy, the authors designed a DNA probe containing a CP (aptamer sequence) and an SP (primer sequence). The CP has two regions, which represent the aptamer sequence of ETEC K88 and the complementary sequence of SP, respectively. Before binding the target, the two probes formed a partial double-strand complex and adsorbed onto GO. This adsorption led to the quenching of the fluorescence of FAM. When the target was added, the probe was released from the GO because of the formation of the target-aptamer complex. SDPR then occurred in the presence of deoxynucleotides (dNTPs) and the KF, displacing the target for binding to another probe and forming numerous dsDNAs repelled by GO. This triggered an increase in fluorescence (Fig. 9A) [149]. The LOD of the established aptasensor for *ETEC K88* detection peaked at 100 CFU/mL. A similar work was also proposed by Liu et al. for analyzing *Salmonella enteritidis* (*S. enteritidis*). By using KF-aided target recycling amplification and exploiting the synergistic effects of FAM and the DNA probe SYBR Green I, the fluorescence was

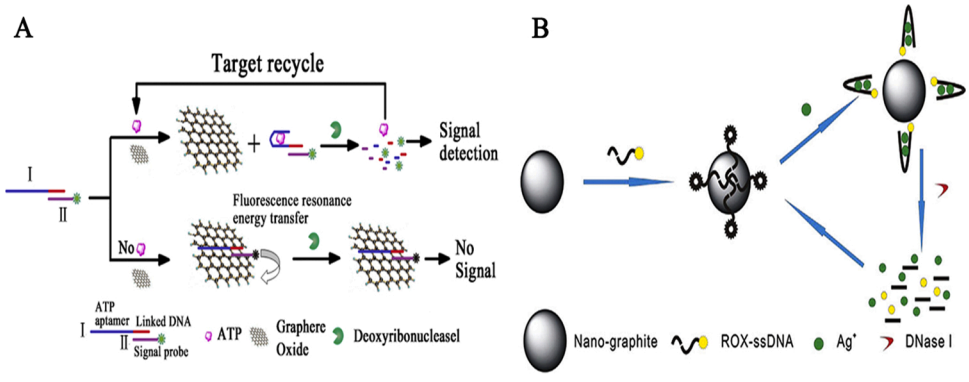

Fig. 8. Aptasensor for bioassay based on DNase I-assisted target recycling. (A) Schematic illustration of the GO-based fluorescent aptasensor for ATP detection by using DNase I-mediated target cyclic amplification. Without ATP, the probe adsorbed onto GO and the fluorescence is quenched. When the ATP is added, the probe dissociated from GO, inducing the increase in the fluorescence intensity. More importantly, the fluorescence is greatly amplified by a DNase I-mediated target recycling process. Fig. 8A adapted from ref. [141]; (B) Schematic illustration of the NG-based aptasensor for Ag^+ based on DNase I-assisted target recycling. Without Ag^+, the C-rich probe adsorbed onto NG and the fluorescence of ROX was quenched. Addition of the Ag^+ triggered formation of C-Ag^+-C complex, causing the enhancement of the fluorescence. Additionally, the DNase I-assisted digestion of the Ag^+-ssDNA complex leaded to the recycling of Ag^+ and accumulation of free ROX fluorophores. Fig. 8B adapted from ref. [145].

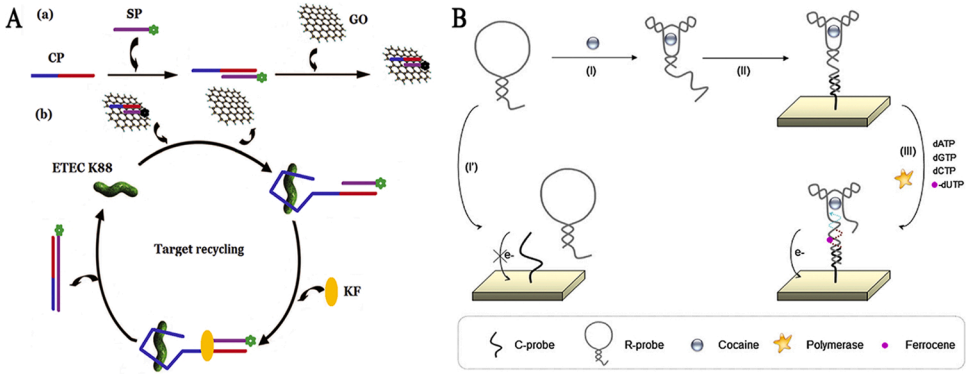

Fig. 9. Aptasensor for bioassay based on KF-assisted target recycling. (A) Schematic representation of a GO-based aptasensor for *ETEC* K88 detection by using KF-aided target cyclic signal amplification. a) Without *ETEC* K88, the probe adsorbed onto GO and the fluorescence of FAM was quenched. b) Recovery and further amplification of the fluorescence after adding targets and the KF. Fig. 8A adapted from ref. [149]; (B) Schematic representation of the electrochemical aptasensor for cocaine detection based on KF extension reaction. In the presence of cocaine, the probe changed its hairpin conformation into the tripartite complex, inducing the occurrence of KF polymerase reaction. Fig. 9B adapted from ref. [150].

significantly amplified and the sensitivity improved. *S. enteritidis* could be assayed in milk samples by this method, with a detection limit of 300 CFU/mL [135]. He et al. reported an electrochemical aptasensor for cocaine detection based on a KF polymerase reaction that combines the aggregation of ferrocene-functionalized oligonucleotide. In the absence of cocaine, the recognition probe (R-probe) maintained its stable hairpin structure, making the complementary fragment of R-probe close so that the CP could not bind with the complementary fragment. In this case, SDPR would hardly occur. When cocaine was introduced, the aptamer could specifically recognize cocaine and the complementary fragment of the R-probe was exposed. This would initiate the SDPR in the presence of KF, forming a longer DNA strand that is complementary to the R-probes. During polymerization, Fc-dUTP was included in the extended primer, which triggered an electrochemical signal change (Fig. 9B) [150]. This sensing platform allowed the detection of cocaine at concentrations as low as 200 μM. An analogous electrochemical aptasensor based on a KF-induced extension reaction was developed for the ultrasensitive detection of platelet-derived growth factor (PDGF) protein. This proposed aptasensor could detect PDGF protein down to 1.8 pM, which makes it a robust biosensing platform for clinical diagnostic applications [151]. Using the KF-based method, other targets, such as adenosine [152], virus [153], and cancer cells [154], were also detected.

3.3.3. *Exonuclease III (Exo III)*

Exo III, a 3′-5′ exonuclease enzyme, does not require a specific enzymatic recognition sequence and can catalyze the stepwise removal of mononucleotides of dsDNA from the blunt or 3′-recessed end. It is inactive toward ssDNA or the protruding 3′-end of a dsDNA longer than four bases. Based on the above properties, the Exo III-assisted target recycling strategy has been employed to develop signal-amplified aptasensor platforms in recent years. Our group designed an aptasensor for the determination of mercury(II) based on the use of GO serving as a nanoquencher and use of Hg(II)-triggered cleavage of the newly formed dsDNA harbored blunt 3′-hydroxyl termini by ExoIII, which induces signal amplification. In this system, three DNA probes, comprising a CP, an SP, and a help probe (HP), were designed, among which the CP and HP were partially complementary to each other. In the absence of Hg(II), CP could block the release of the HP for binding to the SP, leading to FAM-labeled SP being adsorbed onto the surface of GO and quenching the fluorescence of FAM. Upon the addition of Hg(II), the T-rich CP could specifically bind to Hg(II) and form thymidine-Hg(II)-thymidine duplexes, changing the linear structure of CP to a hairpin structure. At the same time, the HP discharged from the CP/HP hybrids would release the SP from the GO and restore fluorescence. The signal was considerably enhanced with the Exo III-assisted targeting and

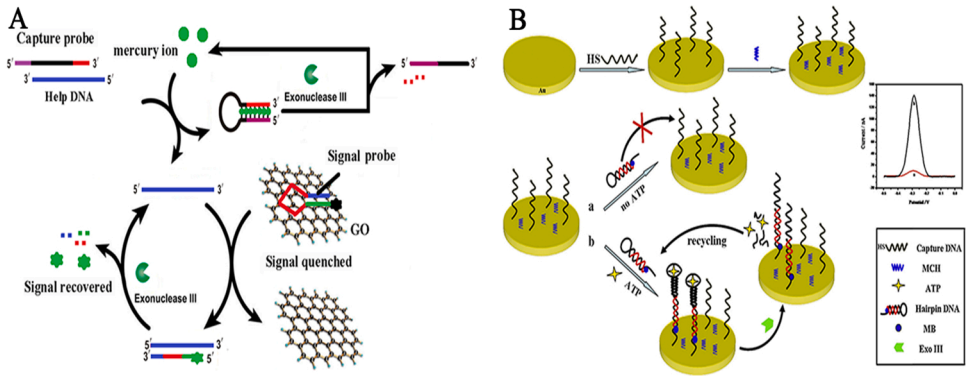

Fig. 10. Aptasensor for bioassay based on Exo III-assisted target recycling. (A) Schematic representation of fluorescence aptasensor for Hg^{2+} based on GO as a nanoquencher and ExoIII as a signal amplifier. Without Hg^{2+}, SP adsorbed onto GO and the fluorescence of FAM was quenched. Upon addition of Hg^{2+}, the linear structure of CP changed to a hairpin structure due to the formation of T-Hg^{2+}-T duplexes. HP is released from the CP/HP hybrids, and this causes SP to be released from GO and fluorescence to be recovered. The signal is strongly amplified by using Exo III-assisted targeting and recycling of HP. Fig. 10A adapted from ref. [155]; (B) Schematic representation of the aptasensor fabrication based on Exo III-assisted target recycling for amplification. Without ATP, the hairpin DNA could not hybridize with the capture DNA, which resisted the cleavage activity of Exo III. With the addition of ATP, ATP aptamer formed G-quadruplex structure with ATP which resulted in structure-switching of the hairpin DNA.Then the hairpin DNA could hybridize with capture DNA and form double-strand structure. As a result, the MB got close to the electrode surface and showed a strong signal. The signal is significantly enhanced by using Exo III-assisted target recycling. Fig. 10B adapted from ref. [156].

recycling of the HP via the accumulation of a large amount of FAM. Therefore, Hg(II) could be assayed by the strong increase in fluorescence (Fig. 10A) [155]. The LOD of this aptasensor used for the Hg(II) assay reached 10 fM. In addition, this strategy was used to assay Hg(II) harbored in three Chinese medicines and prominent results were also achieved. Bao et al. constructed an electrochemical aptasensor for the sensitive detection of ATP based on exonuclease III-aided target recycling for signal amplification. They designed a hairpin DNA containing an aptamer sequence labeled with methylene blue (MB) at its 5′-end, and its 3′-end had six bases overhanging to form a hairpin conformation. In the absence of ATP, the hairpin DNA could not hybridize with the capture DNA because the red region in the hairpin is closed by the aptamer sequence, and the 3′-end still retains the single-strand structure, which allows it to resist the cleavage of Exo III. In the presence of ATP, the ATP aptamer binds to ATP, resulting in the red region being exposed for hybridization with capture DNA and forming a dsDNA structure at the 3′-end simultaneously. Therefore, MB was close to the electrode surface and displayed an obvious signal. Importantly, Exo III could cleave the double strand from the 3′-end, leading to the release of ATP. The released ATP would recognize other hairpins to enter the next recycling process (Fig. 10B) [156]. The proposed electrochemical aptasensor could detect ATP with a detection limit of 34 pM. Other targets, including cytokines [157], MUC1 [158], lysozyme [159], and ochratoxin A [160], were also assayed based on Exo III-assisted signal amplification using different design strategies. However, Exo III can only implement the enzymatic activity of digesting the double strand from the 3′-end, so designers must fabricate methods to meet its unique property, restricting its applications to some extent.

3.4. Split aptamer designs

It is interesting that when an aptamer splits into two pieces, equilibrium is displayed between its two dissociated parts and the target. If the target binds the two fragments with high affinity, the presence of the target will induce the equilibrium toward the formation of a sandwich structure (apt1-target-apt2) via self-assembly, changing the signal. Hence, the accuracy of the target assay can be significantly improved by employing two split aptamers instead of a single aptamer to recognize the target with high specificity. Using these advantages, numerous aptasensors based on sandwich assays have been created for the determination of various targets by splitting the aptamer into two fragments. Bai et al. developed a fluorometric aptasensor for the determination of 19-nortestosterone (NT). A 76-mer aptamer of 17β-estradiol was split into two pieces, P1 and P2, where P1 was labeled with a quencher (BHQ) and P2 with a fluorophore (6FAM). In the absence of the target, P1 and P2 were far away from each other, and strong fluorescence could be measured in the detection system. In contrast, the fluorescence sharply decreased after P1 and P2 were bound to the target simultaneously by proximity-dependent FRET (Fig. 11A) [161]. Additionally, the authors found an interesting phenomenon: the sensitivity for NT was higher than that for 17β-estradiol in this proposed design. It is likely that the BHQ and FAM were closer in the P1-NT-P2 complex than in the P1-17β-estradiol-P2 complex. Zhou et al. created a split aptamer-based sensor for the determination of ATP via SERS. They designed two split aptamers attached to two SERS substrates that were used for the specific recognition of ATP. Apt1 was immobilized onto gold nanoparticle-decorated graphene oxide (GO/Au3) and Apt2 onto gold nanoparticles (Au2). Before the addition of ATP, different elements in this system did not connect with each other, and a low signal existed in this platform. When ATP was introduced, Apt1 and Apt2 were bridged by forming a sandwich structure that led to the GO/Au3 nanolayer and the Au2 nanoparticle being in close proximity. Accordingly, the SERS signal was greatly restored (Fig. 11B) [162]. Based on this design, HIV-1 Tat protein [163], cocaine [164], and tumor cells [165] were also detected by different research groups. To construct an effective split aptasensor, some important issues still need to be considered, such as the choice of the splitting site and the aptasensor retaining its binding activity and affinity.

4. Aptamer-based targeted therapy

4.1. General

Many drugs used for clinical treatment do not precisely discriminate between diseased cells and normal cells, which means that these drugs not only display toxicity toward pathological cells but also have adverse effects on normal cells. Therefore, it is of great importance to implement selective and efficacious therapies with minimal toxicity. In recent years, targeted therapy has attracted much attention owing to its selectivity and efficiency. Targeted therapy can promote the specificity of delivered drugs or biological agents for a predetermined position and increase their accumulation in diseased tissue cells, aiming to enhance the selectivity of therapeutic effects and reduce adverse effects [166, 167]. One strategy toward this goal is to use target-specific ligands to load the less-specific therapeutics, such that the drugs can be delivered selectively to pathological tissues or organs. Among these ligands, aptamers can specifically bind to disease biomarkers, making them promising candidates targeted therapy [168,169]. We will discuss three categories: aptamers as therapeutics, aptamer-drug conjugated systems, and aptamer-nanomaterial conjugated systems.

4.2. Aptamers as therapeutics

4.2.1. Aptamers as therapeutics for infectious diseases

An inhibitory aptamer that can impair the function of the target protein can be used directly as a therapeutic antagonist. Biofilm formation is an important cause of multiple-drug resistance and persistent infection in clinical settings. Motility and initial attachment assisted by flagella are required for biofilm formation [170]. Hence, suppressing the flagella function is a possible approach to hamper biofilm formation.

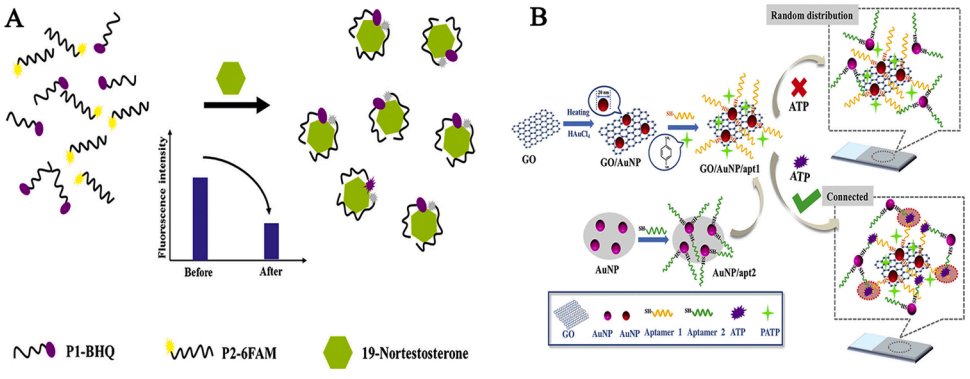

Fig. 11. Split aptamer-based designs. (A) Schematic illustration of homogeneous detection of 19-nortestosterone using a split aptamer-based sandwich-format FRET assay. Addition of 19-nortestosterone leaded to the formation of sandwich structure, triggering the fluorescence quenching between BHQ-labeled P1 and FAM-labeled P2 due to FRET. Fig. 11A adapted from ref. [161]; (B) The schematic illustration of the sandwich assay SERS detection of ATP based on the GO/AuNP/apt1 nanolayer and AuNP/apt2. Addition of ATP leaded to the formation of sandwich structure, triggering the SERS signal enhancement due to the GO/Au3 nanolayer and the Au2 nanoparticle close to each other. Fig. 11B adapted from ref. [162].

Ning et al. screened aptamer 3, which that can target the functional domains of flagellin of *Salmonella choleraesuis* (*S. choleraesuis*), causing the suppression of tropism and initial attachment (Fig. 12A) [171]. After treatment with aptamer 3, the quantity of the biofilm in the presence of aptamer 3 was considerably lower than that in the absence of aptamer 3, indicating that the biofilm-forming ability of *S. choleraesuis* was significantly blocked by aptamer 3. In addition, upon pretreatment with aptamer 3, few ampicillin was required to achieve the same rate of inhibition, preventing the generation of antibiotic-resistant strains. Therefore, aptamer 3 exhibits great potential to be developed as an inhibitor of biofilm formation, which makes it sense in reversing bacterial resistance and combating persistent infection in clinical settings. The hemagglutinin (HA) protein of influenza virus is a trimeric spike on the viral envelope that is responsible for hemagglutination and adsorption onto susceptible host cells. This adsorption mediates the subsequent entry of influenza viruses into host cells via membrane fusion, which is significant for initial viral infection [172]. Hence, HA may be a potential target for influenza virus therapy by inhibiting its function. Li et al. selected aptamer 1, which is specific to the HA protein of the H1N1 influenza virus (A/Puerto Rico/8/1934) to inhibit the virus-induced hemagglutination of chicken RBCs and block its proliferation in MDCK cells [173]. The results of hemagglutination inhibition assay and microneutralization assay showed that the binding of aptamer 1 to the HA protein is critical for the inhibition of HA-receptor (glycan) interactions, which could inhibit its adsorption and proliferation in the host cells (Fig. 12B). Research on a similar working mechanism has also emerged in the treatment of AIDS. The gp120 protein of HIV interacting with its primary receptor CD4 plays an important role in attaching to the CD4+ cell surface that is necessary for viral entry. Many aptamers against gp120 have been obtained to neutralize the HIV infection by blocking the binding between gp120 and CD4. The first anti-HIV aptamer, named ISIS 5320, was proposed by Wyatt et al. in 1994. [174]. The authors selected a phosphorothioate 8-mer d($T_2G_4T_2$) that could suppress viral entry by forming a parallel-stranded tetrameric guanosine-quartet structure that could bind to the V3 loop of gp120. In 2009, Zhou screened 2′-F-pyrimidine-substituted RNA aptamers against gp120 and showed that they neutralized infectivity in cultured CEM T-cells and primary blood mononuclear cells (PBMCs) [175]. These aptamers displayed no toxicity, low usage, and high efficacy, suggesting that they may have great promise for further development as a HIV-1 entry inhibitor. In addition to the aptamers against gp120, other aptamers against reverse transcriptase [176], integrase [177], protease [178], and Gag protein [179] were also used to block HIV from replicating in the host, making them good prospects for treating AIDS in a clinical setting. Several aptamers have been developed as therapeutics for the treatment of viral infections, such as aptamers against severe acute respiratory syndrome coronavirus (SARS-CoV) [180], human papilloma virus (HPV) [181], and Ebola virus [182]. Overall, the use of these aptamers as therapeutic drugs is a promising alternative for the treatment of infectious diseases.

4.2.2. *Aptamers as therapeutics for cancers*

Recently, aptamers used for cancer treatment have also been developed as therapeutic agents. AS1411, the most successful aptamer for cancer treatment, is an unmodified guanosine-rich 26-mer DNA sequence that was the first aptamer to enter clinical trials for cancer treatment [183]. AS1411, which was discovered fortuitously in the process of screening antiproliferative DNA oligonucleotides, instead of the SELEX process, could specifically bind with nucleolin by forming a stable G-quadruplex structure. Nucleolin is highly expressed on the surface of many cancer cells and is closely related to cell growth, proliferation, and survival. After binding to nucleolin, AS1411 was then internalized into the cells and the aptamer-nucleolin complex aroused the inhibition of DNA replication [184,185]. Soundararajan et al. further discovered that AS1411 could significantly reduce the stability of BCL-2 mRNA and promote cell apoptosis through cytotoxicity [186]. Girvan et al. found that AS1411 could inhibit cell proliferation by blocking the NF-κB signaling pathway, which led to the arrest of cells in the S phase [187]. Although some potential mechanisms of AS1411 action have not been fully elucidated, AS1411 still shows a huge advantage in inhibiting the proliferation of tumors. Prostate-specific membrane antigen (PSMA) is a transmembrane protein that is overexpressed in prostate cancer (PC) cells. Because of its overexpression, PSMA is a potential biomarker for the targeted therapy of PCs. It is reported that PSMA plays a critical role in prostate cancer progression by executing enzymatic activity [188]. Dassie et al. developed an RNA aptamer (A9g) against PSMA that could inhibit the enzymatic activity of PSMA, diminishing PC cell migration/invasion in vitro. In addition, A9g was confirmed to be safe and nontoxic in vivo, which enabled its development as a novel RNA smart drug for PC treatment [189]. Human epidermal growth factor receptor 2 (HER2), a member of the EGFR family, is a receptor tyrosine kinase that is expressed in a variety of cancers, including breast and gastric tumors. Mahlknecht et al. selected a 42-nt DNA aptamer targeting HER2 by SELEX using HER2-specific polyclonal antiserum. After the 14-nt aptamer was obtained, the authors designed a trimeric version (42 nt) to enhance the binding affinity to HER2 and improved the internalization of HER2 owing to the formation of multimolecular complexes at the cell surface. After treatment with the trimeric aptamer, the growth of the gastric cancer cells was inhibited by accelerating the lysosomal degradation of the target protein. Moreover, the tumor volume in HER-2-positive immunocompromised mice was greatly reduced via intraperitoneal injection of the trimeric aptamer [190]. In addition to the above-mentioned tumor-specific aptamers, some other aptamers against different types of cancer cell biomarkers, including AX102 targeting platelet-derived growth factor (PDGF)-B chain [191], Gint4.T targeting platelet-derived growth factor receptor-β (PDGFR-β) [192], and NOX-A12 targeting CXC chemokine ligand 12 (CXCL12) [193], were also isolated for cancer treatment by inhibiting cell migration and proliferation, inducing cell differentiation, impeding tumor growth in vivo, or downregulating signaling pathways associated with tumor activation. In addition to using aptamers for their direct impact on cancer cells for cancer therapy,

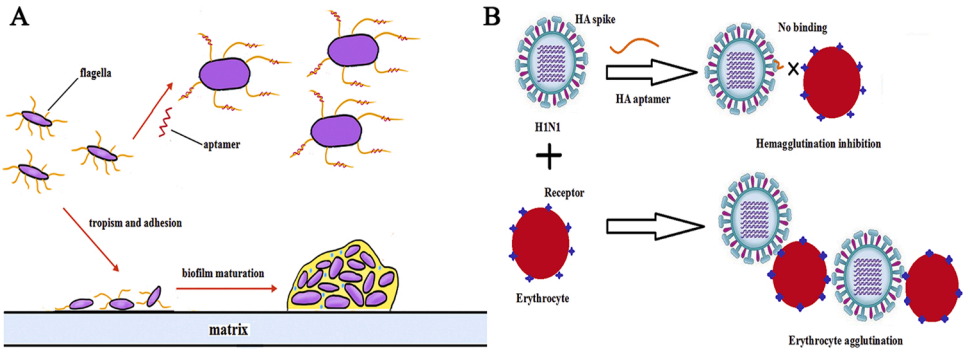

Fig. 12. Aptamer used for combating infectious diseases. (A) The aptamer used for suppressing the biofilm formation on an abiotic surface at the early stage. Flagella-mediated motility makes the cells initial contacts with a matrix and forms mature biofilms in absence of aptamer 3. Upon adding aptamer 3, the tropism and early attachment mediated by flagella were suppressed. Fig. 12A adapted from ref. [171]; (B) The aptamer used for inhibiting erythrocyte agglutination. The binding of HA to its receptor can cause erythrocyte agglutination in absence of aptamer 1. Addition of aptamer 1 could suppress erythrocyte agglutination by interfering with HA-glycan interactions.

they can also be developed as a regulator of the immune system that can inhibit cancer cell growth indirectly. 4-1BB is a major costimulatory receptor that can promote the survival and expansion of activated T cells, which play an important role in promoting the generation of protective antitumor immune responses. McNamara et al. selected aptamers targeting 4-1BB and used multivalent aptamers to enhance $CD8^+$ T cell proliferation and cytolytic activity, aiming to inhibit tumor growth in mice [194]. This study provides a possible new avenue for cancer therapy of manipulating the immune system by activating the functions of aptamers.

4.2.3. Aptamers as therapeutics for other human diseases

Therapeutic aptamers have also been expanded to other human disease treatments. Pegaptanib, the first therapeutic aptamer approved by the US FDA as an anti-angiogenic medicine, is a 27-nt RNA aptamer that specifically binds to VEGF, which can cure neovascular age-related macular degeneration (AMD) by blocking intraocular blood vessel growth [195]. NOX-H94 is a 44-nt RNA aptamer that specifically binds to hepcidin. This binding blocks hepcidin-regulated ferroportin degradation and reversed hyperferremia activity, which makes it a potential therapeutic strategy for the treatment of anemia of chronic inflammation [196]. ARC1779 is a 49-nt DNA/RNA aptamer that binds specifically to von Willebrand factor (vWF), resulting in the inhibition of platelet activation and pathological thrombosis by blocking the vWF-mediated activation pathway [197]. The development of these aptamers not only provides new alternatives for different kinds of human disease treatment, but also expands the strategies for treating human diseases.

4.3. Aptamer-drug conjugate (ApDC) systems

4.3.1. Aptamer-chemotherapeutical drug conjugates

Aptamers can not only be selected to target and treat a variety of human diseases, but they can also be used for targeted cytotoxic drug delivery. The direct use of cytotoxic drugs is restricted by their adverse effects on normal cells and low maximum tolerated dosage owing to the off-target effects. Owing to the high specificity of the aptamers, the preparation of aptamer-cytotoxic drug complexes via non-covalent or covalent conjugation methods can fulfill cytotoxic drug targeted delivery, which will increase the accumulation rate of the drug in target cells and reduce the adverse effects. Doxorubicin (Dox), an anticancer drug that can inhibit DNA replication and transcription by inserting itself into the double-stranded CG sequences of DNA and RNA, is the most widely used chemotherapeutic drug for treating many cancer types, such as cell acute lymphoblastic leukemia, breast cancer, and malignant lymphomas [198,199]. Dox can lead to cardiotoxicity, including dilated cardiomyopathy and congestive heart failure, which makes it possible to develop targeted Dox-delivery systems [200]. Bagalkot et al. surveyed the targeted delivery of Dox to PC cells by employing the PSMA aptamer A10. Dox molecules were non-covalently intercalated in the double-stranded region of A10 and formed an aptamer-Dox complex (Fig. 13A) [201]. When it was used to treat the target cells, the conjugate was assimilated into PC cells via internalization mediated by specific binding between A10 and PSMA, followed by the intracellular release of Dox. To promote the loading capacity and therapeutic effect of Dox, Macdonald et al. designed a bifunctional aptamer-Dox conjugate that is capable of penetrating the blood-brain barrier and specifically delivering its cytotoxic payload to epithelial cell adhesion molecule-positive brain metastases. The secondary structure of this aptamer consisted of two hairpin structures, allowing more Dox to be inserted into the stem regions, which will enhance the drug payload and therapeutic efficiency (Fig. 13B) [202]. Although the non-covalent method is simple and efficient, it still has some flaws. For example, drugs probably dissociate from aptamers before they bind to the targeted cells or tissues. This issue can be addressed by covalent conjugation between drugs and aptamers. Huang et al. conjugated Dox to a DNA aptamer named sgc8c using a hydrazone linker for the specific killing of target cells (Fig. 13C) [203]. sgc8c can recognize protein tyrosine kinase 7 (PTK7), which is highly expressed in T-cell acute lymphoblastic leukemia (TALL) cells. The Dox-sgc8c conjugate could be efficiently internalized by TALL cells via binding to PTK7. After internalization, Dox could be released from the conjugate in lysosomes (pH 4.5–5.5) owing to the pH-sensitive covalent linkage between Dox and sgc8c. However, only a few drugs can be conjugated onto one aptamer in ApDCs, resulting in a low drug loading

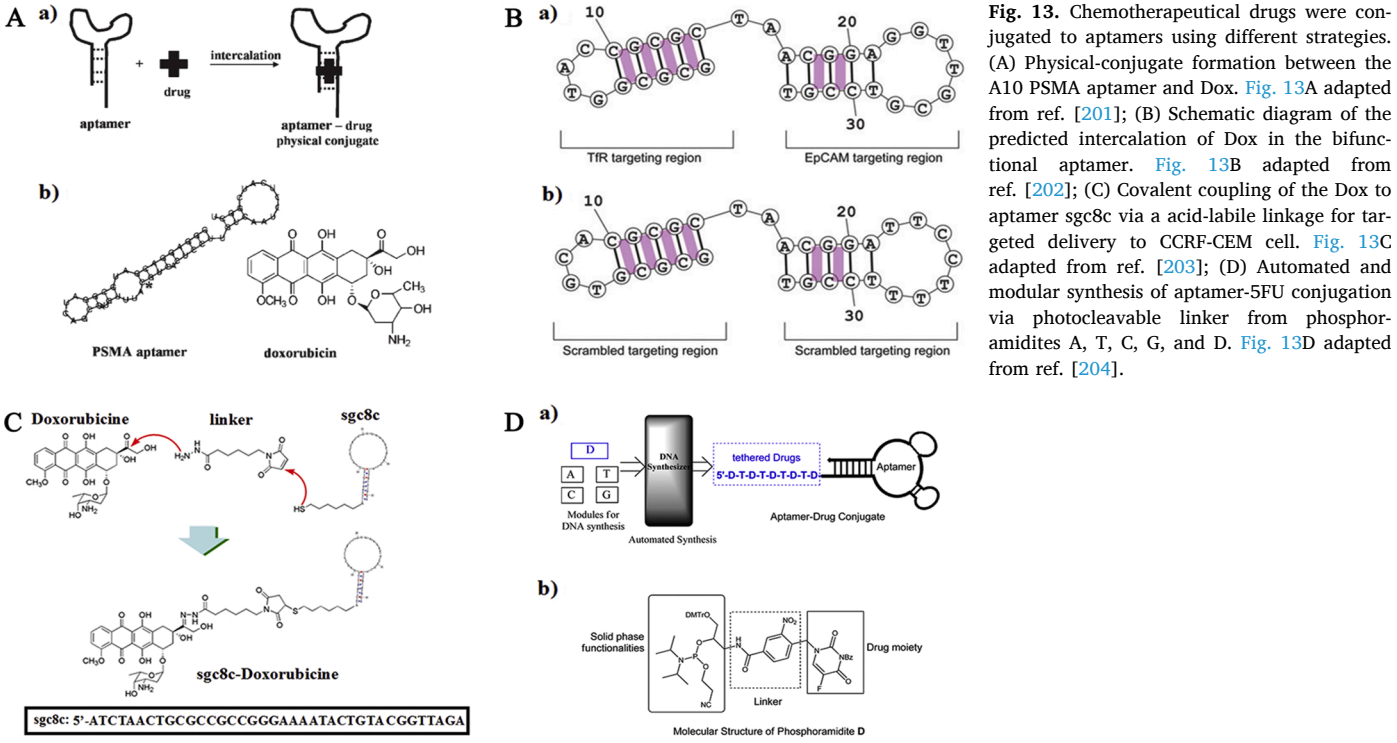

Fig. 13. Chemotherapeutical drugs were conjugated to aptamers using different strategies. (A) Physical-conjugate formation between the A10 PSMA aptamer and Dox. Fig. 13A adapted from ref. [201]; (B) Schematic diagram of the predicted intercalation of Dox in the bifunctional aptamer. Fig. 13B adapted from ref. [202]; (C) Covalent coupling of the Dox to aptamer sgc8c via a acid-labile linkage for targeted delivery to CCRF-CEM cell. Fig. 13C adapted from ref. [203]; (D) Automated and modular synthesis of aptamer-5FU conjugation via photocleavable linker from phosphoramidites A, T, C, G, and D. Fig. 13D adapted from ref. [204].

capacity. To overcome these challenges, Wang et al. designed and synthesized a therapeutic module for solid phase synthesis, which is a phosphoramidite containing an anticancer drug moiety and a photocleavable linker (Fig. 13D) [204]. Using these ApDCs, multiple copies of drugs can be site-specifically conjugated onto each aptamer molecule, which greatly increases the drug loading capacity. Taken together, aptamer-drug conjugates designed by non-covalent or covalent methods can not only promote the anticancer effect compared to unconjugated drugs, but also display low cardiotoxicity and general limited toxicity toward non-target cells both in vitro and in vivo.

4.3.2. *Aptamer-small interfering RNA (siRNA) conjugates*

SiRNA, also called silencing RNA, is a powerful tool that offers the possibility to silence the expression of specific genes owing to its broad applicability and high efficiency, paving the way for precise medicine. SiRNA is 20–25 nucleotides that can cause the degradation of target mRNA through the formation of the RNA-induced silencing complex (RISC) [205,206]. Although researchers have demonstrated the mechanisms and merits of RNAi, this method still faces many challenges in its clinical application. The most serious issue is the lack of safe and effective tools for RNAi-specific delivery. The attractive properties of aptamers make them prominent candidates for the targeted delivery of siRNA. Mcnamara et al. first developed covalently linked aptamer-siRNA chimeric molecules to specifically deliver therapeutic siRNAs targeting PLK1 and BCL2, two survival genes that are overexpressed in most human cancers. After binding the PSMA, siRNAs were internalized and cleaved by Dicer, leading to silencing of the target mRNA and apoptosis in a xenograft model of prostate cancer (Fig. 14A) [207]. To increase the loading capacity and therapeutic efficiency, Liu et al. attempted to design an RNA-based aptamer-siRNA chimera, which is composed of a bivalent aptamer that specifically binds PSMA to induce siRNA internalization in PC cells and two siRNAs targeting EGFR and survivin, which are covalently fused between two aptamers (Fig. 14B) [208]. Since the two aptamers against PSMA are capable of loading two different types of siRNA, the chimera can inhibit EGFR and survivin simultaneously and induce apoptosis effectively, which will significantly suppress tumor growth and angiogenesis. Besides the direct inhibition of tumor growth or induction of apoptosis by silencing-related gene expression, the activation of anti-tumor immunity is also a good approach for cancer treatment. Signal transducer and activator of transcription 3 (STAT3) is a key downstream effector oncogene that can always be activated in many cancer types. Hence, it is a promising target for cancer treatment. Kortylewski et al. fabricated a DNA aptamer-siRNA conjugate that combines targeted siRNA delivery and the activation of immune cells by covalently linking toll-like receptor 9 (TLR9) oligonucleotide agonist aptamer (CpG 1668) to siRNAs. After binding to TLR9, the siRNA was internalized by the target cell and disposed of by Dicer, resulting in the suppression of STAT3 expression and activation of antitumor immunity in the tumor microenvironment [209]. Zhou et al. developed an RNA aptamer-siRNA conjugate to inhibit STAT3 expression. The aptamer against the B-cell-activating factor (BAFF) receptor (BAFF-R) was linked to a siRNA directed against STAT3 by either covalent or non-covalent conjugation. The RNA aptamer in this conjugate not only blocks BAFF-mediated B-cell proliferation, but also induces the internalization of siRNA to silence target mRNA. Therefore, the dual-functional BAFF-R aptamer-siRNA conjugates are able to deliver siRNAs and block ligand-mediated processes, making them promising for B-cell malignancy treatment [210]. The aptamer-siRNA conjugates were also used to combat AIDS. Zhou et al. developed aptamer-siRNA chimeras for the cell type-specific delivery of siRNAs in a HIV-1 infected RAG-hu mouse model. The aptamer targeting gp120 was covalently conjugated to siRNAs targeting the HIV-1 tat/rev gene. gp120 expressed on the surface of HIV-1-infected cells permitted binding and internalization of the aptamer-siRNA chimeric molecules by endocytosis. After the conjugates are taken up by the target cell, the linked siRNA is processed by Dicer followed by the release of an anti-tat/rev siRNA for the specific silencing of the targeted mRNA transcript. In addition to silencing the target gene expression by siRNA, the aptamer selectively bound to gp120 can block the gp120-CD4 receptor interaction. Accordingly, this anti-gp120 aptamer-siRNA conjugate possesses a dual inhibitory function. Moreover, the silencing potency can be enhanced when the length of the siRNA is increased from 21 to 27 bp, probably

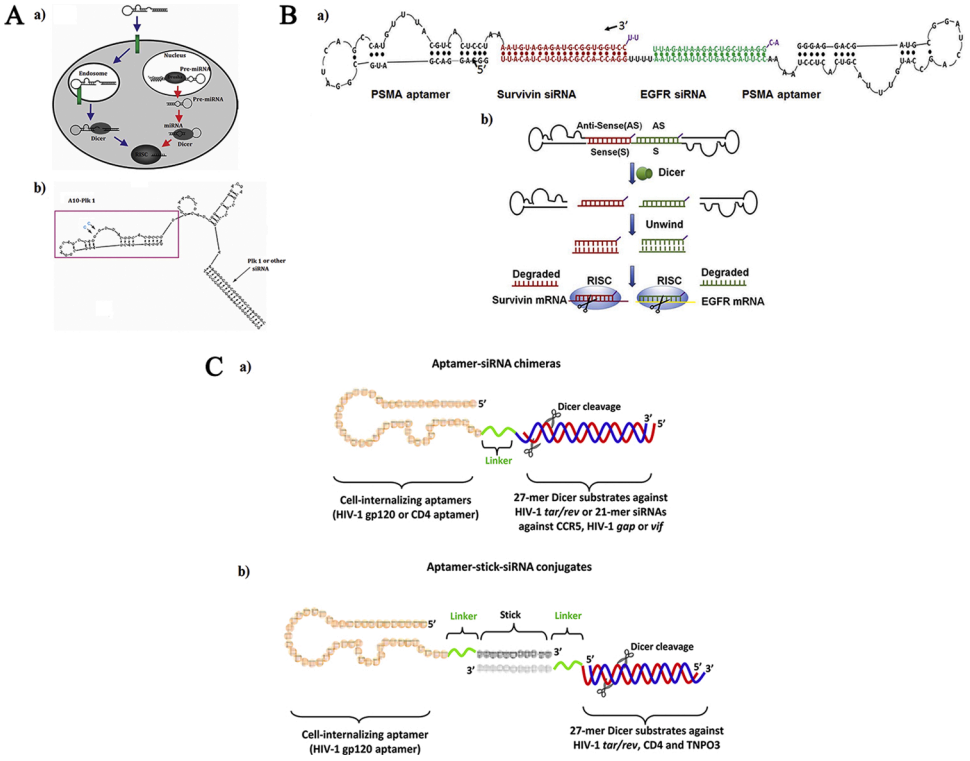

Fig. 14. SiRNAs were conjugated to aptamers using different strategies. (A) Aptamer-siRNA chimeras were synthesized via covalent conjugation. The aptamer-siRNA chimera is endocytosed, and subsequently released from the endosome to enter the RNAi silencing pathway. Fig. 14A adapted from ref. [207]; (B) Aptamer-siRNA chimeras consist of a bivalent PSMA aptamer and two siRNAs specific to survivin and EGFR, respectively. Upon internalization, Dicer will process chimera into 21-nt siRNA duplex, inducing targeted mRNA silencing. Fig. 14B adapted from ref. [208]; (C) Aptamer-siRNA chimeras (a) and aptamer-stick-siRNA conjugates (b) for inhibiting HIV. Fig. 14C adapted from ref. [212].

because the Dicer processing of the 27-mer from the aptamer generates a more efficient RISC. [211]. This group also designed a sticky bridge strategy by non-covalently conjugating the aptamer with three different siRNAs against the HIV-1 tat/rev gene, CD4 molecule, and transportin 3. In this design, the two complementary sequences in the GC-rich sticky bridge were covalently attached to the 3′-end of the aptamer and one of the two siRNAs, respectively. Linker structures were added as spacers between the aptamer and siRNA to allow for spatial and structural flexibility. After the specific binding and internalization of the aptamer-siRNA conjugates into target cells, the aptamer-sticky bridge--siRNA complexes also acted as dual-function inhibitors that can down-regulate targeted gene expression and suppress HIV replication (Fig. 14C) [212]. Compared to that of aptamer-siRNA conjugates, the cost of chemical synthesis of the aptamer-sticky bridge-siRNA complexes is lower. Furthermore, this sticky bridge-based strategy can be used to easily link different siRNAs to a single aptamer, which will prevent the virus from developing resistance to the siRNA component.

4.4. Aptamer-nanomaterial conjugated system

4.4.1. QDs

QDs, also known as nanoscale semiconductor nanocrystals, have captured the fascination and attention of researchers owing to their unique optical properties, such as a high quantum yield, resistance to photobleaching, and broad absorption with narrow photoluminescence spectra, which makes it a potential drug delivery vehicle [213,214]. Bagalkot et al. developed a novel QD-Apt conjugate to be loaded with Dox for the targeted delivery of drugs to PC cells based on the mechanism of binary (Bi)-FRET (Fig. 15A) [215]. The conjugate consists of three components, including QDs that act as fluorescent imaging vehicles, the A10 PSMA aptamer covalently linked to QDs using EDC/NHS chemical coupling that serves as recognition elements and Dox carrying vehicles, and Dox, which intercalates into double-stranded CG sequences of the aptamer as a therapeutic agent. In this conjugate, the fluorescence of the QD was quenched by Dox, while the fluorescence of Dox was simultaneously quenched by a double-stranded RNA aptamer. After endocytic uptake of the conjugate into the target cell, Dox is gradually released from the conjugate, leading to the simultaneous restoration of Dox and QD fluorescence. Hence, this multifunctional delivery system not only delivers Dox to the targeted cells, but also senses the delivery of Dox by inducing the fluorescence of QDs. In addition, the authors confirmed that the cytotoxicity of this conjugate was almost identical to that of free Dox. Savla et al. designed a pH-responsive QDs-mucin 1 aptamer-Dox (QD-MUC1-DOX) conjugate for the chemotherapy of ovarian cancer (Fig. 15B) [216]. In contrast to the above conjugate, the mucin 1 aptamer and Dox were all linked to the QD in this design. QD was conjugated with a DNA aptamer via EDC/NHS catalysis that could specifically recognize mutated MUC1 mucin over-expressed in ovarian cancer cells. Dox was coupled to the QD via a pH-sensitive hydrazone bond, aiming to maintain the stability of the conjugate and implement drug release in an acidic environment inside cancer cells. After the conjugate was taken up by ovarian cancer cells, Dox was released from the QD-Dox conjugate in an acidic environment to destroy cancer cells. The authors have proven that the developed QD-MUC1-DOX conjugate had higher cytotoxicity than did free Dox in multidrug-resistant cancer cells and specifically accumulated in target cells. Although QDs can not only act as nanocarries for targeted drug delivery, but also as tools for bioimaging in vivo, they may also pose adverse effects on human health and the environment under certain conditions due to their potential toxicity. Therefore, the studies investigated by different research groups showed that extremely low concentrations of QDs may be sufficient to produce obvious effects for biomedical applications [217,218].

4.4.2. Gold nanoparticles

Gold nanoparticles (Au NPs or GNPs) have attracted great interest in the research community because of their extraordinary physical and chemical properties, including low cytotoxicity, excellent biocompatibility, high cell uptake capability, easy biomolecule modifications, and shape- and size-dependent optical and electronic properties [219,220]. These beneficial characteristics of Au NPs enable them to be used as carriers for a variety of therapeutics. Luo et al. developed an aptamer/hairpin DNA-Au NP (apt/hp-Au NP) conjugate for the targeted delivery of Dox for TALL treatment (Fig. 16A) [221]. The DNA aptamer sgc8c, which was used as a recognition ligand for PTK7, was assembled onto the surface of Au NPs, and the hairpin DNA on the Au NP surface was used for loading the anticancer drug Dox. The results obtained from flow cytometry and atomic absorption spectroscopy clearly demonstrated that the aptamer-functionalized nanoconjugates were specific for capturing target cancer cells. After the conjugate was taken up into the

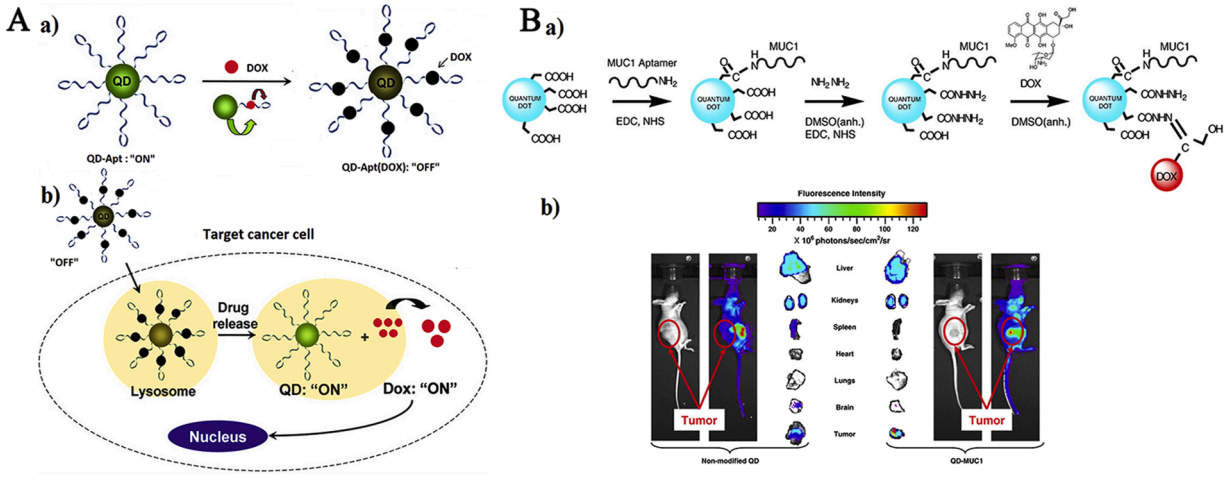

Fig. 15. Aptamer-QDs-drugs conjugated system. (A) Schematic illustration of QD-Apt(Dox) Bi-FRET system. a) The CdSe/ZnS core-shell QD was functionalized with A10 PSMA aptamer followed by the intercalation of Dox, leading to quenching of both QD and Dox fluorescence through a Bi-FRET mechanism. b) Specific uptake of QD-Apt(Dox) conjugates into target cancer cell through PSMA mediate endocytosis could induce the release of Dox from the QD-Apt(Dox) conjugates, causing the recovery of fluorescence from both QD and Dox. Fig. 15A adapted from ref. [215]. Copyright (2007) American Chemical Society; (B) Synthesis of quantum dot-MUC1 aptamer doxorubicin (QD-MUC1-Dox) conjugate. a) Carboxyl-terminated QD was conjugated with MUC1, then Dox was loaded onto the QD-aptamer conjugate and formed the QD-MUC1-Dox conjugate. b) Organ and tumor content of non-modified quantum dots (QD) and tumor-targeted by MUC1 aptamer QD (QD-MUC1) conjugate. Fig. 15B adapted from ref. [216].

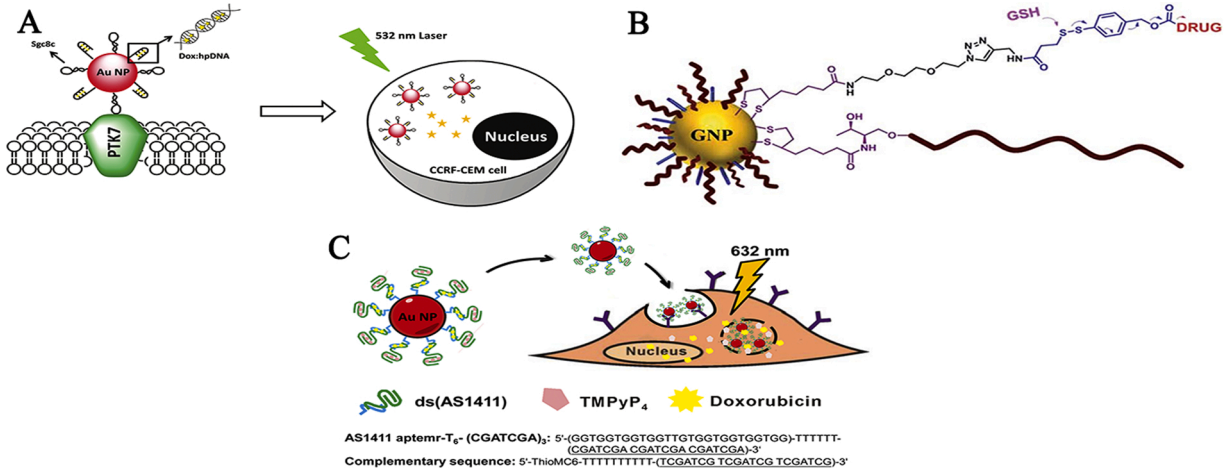

Fig. 16. Aptamer-Au NPs-drugs conjugated system. (A) Light-induced Dox release from Dox:apt/hp-Au NP nanocomplexes inside targeted cancer cells. Aptamers or hairpin DNAs loaded with Dox were conjugated to Au NPs via Au-S linker. Upon internalization, laser could assist the release of Dox molecules from the Dox-loaded drug carrier. Fig. 16A adapted from ref. [221]. Copyright (2011) American Chemical Society; (B) Schematic representation of DNA functionalized GNPs loaded with drug. Aptamer is conjugated via a dithiolane linker. The drug is conjugated through a bifunctional linker composed of an anchoring dithiolane moiety and self-immolative spacer. The release of Dox or AZD8055 is triggered by GSH breaking the disulfide group. Fig. 16B adapted from ref. [222]; (C) Schematic illustration of the co-drugs delivery platform based on aptamer-functionalized Au NPs. The aptamers were conjugated to Au NPs followed by the intercalation of Dox and TMPyP4. Light induced the release of Dox and TMPyP4. Fig. 16C adapted from ref. [223]. Copyright (2014) American Chemical Society.

target cells, Dox was released from the Dox-loaded drug carrier with the assistance of photoenergy and the accompanying local photothermal heating response induced by illumination with a continuous-wave (CW) laser. Additionally, the nanoconjugates displayed enhanced antitumor efficacy with few side effects when illuminated with plasmon-resonant light at 532 nm. Latorre et al. designed an aptamer/Au NPs/drug conjugate by covalent modification (Fig. 16B) [222]. The aptamer AS1411 was conjugated to Au NPs through a dithiolane linker, and the drug (Dox or AZD8055) was conjugated to Au NPs through a bifunctional linker composed of an anchoring dithiolane moiety and a self-immolative spacer. After the conjugate entered into the target cells, the drug was released in the presence of glutathione (GSH) due to the cleavage of the disulfide group, which could promote electronic movement by the π cloud, rendering the release of CO_2 and the therapeutic in a 1,6-benzyl elimination reaction. To improve the therapeutic efficacy and reduce the development of drug resistance, Shiao et al. devised an aptamer-functionalized Au NP to co-deliver two different anticancer drugs to improve the drug effectiveness (Fig. 16C) [223]. The AS1411 aptamers were linked to Au NPs via strong gold–thiol linkages, and then TMPyP4 and Dox were physically inserted into the AS1411-conjugated Au NPs, leading to the formation of the T/D:ds-NPs conjugate. After the conjugate penetrated into tumor cells, such as HeLa and Dox-resistant MCF-7R cell lines, reactive oxygen species induced by TMPyP4 molecules were generated when illuminated at 632 nm light, resulting in cell damage. At the same time, Dox was released from this conjugate during the photodynamic reaction. Importantly, the toxicity of this co-drug conjugate toward the target tumor cells was advantageous over individual drug treatments. Although Au NPs display good merits for targeted drug delivery, the accumulation and potential long-term toxicity of AuNPs have not yet been studied. Moreover, the high costs of large-scale production remain a challenge.

4.4.3. *Carbon nanomaterials*

Many carbon nanomaterials, including single-walled carbon nanotubes (SWCNTs), GO, fullerene, and carbon dots (CDs) have recently been used in the biomedical field. Among these, SWCNTs and GO have been extensively investigated as promising delivery vehicles for targeted drug delivery because of several important properties, such as good biocompatibility, cheap preparation, and a large surface area for linking specific targeting molecules via either covalent or non-covalent modification [224,225]. Zhang et al. fabricated a multifunctional tumor-targeting drug delivery system by using SWCNTs as a drug delivery vehicle, AS1411 as a recognition element, and Dox as a model chemotherapy drug. SWCNTs were first modified with F68 to promote its water dispersion and biocompatibility. Dox was then added and could be easily absorbed onto SWCNTs via π-π stacking, electrostatic adsorption, and hydrophobic interactions. Finally, AS1411 was coupled to the formed Dox-SWCNTs by π-π stacking and electrostatic adsorption to obtain an AS1411-Dox-SWCNTs delivery system. This conjugate not only maintained both the cytotoxicity of Dox and the optical properties of SWCNTs, but also enhanced their accumulation in tumor cells, endowing this conjugate with dual chemotherapy and photothermal therapy functions [226]. Taghavi et al. also constructed a multifunctional tumor-targeting drug delivery system combining the selected shRNAs with Dox by using SWCNT via covalent coupling. Carboxylated SWCNTs modified with polyethylenimine (PEI) through a polyethylene glycol (PEG) linker was used as a vehicle for shRNA delivery (Fig. 17A) [227]. The AS1411 aptamer was covalently linked to the shRNA-SWCNT-PEG-PEI conjugate, followed by the intercalation of Dox with pBcl-xL shRNA-SWCNT-PEG-PEI-Apt. This conjugate could not only implement shRNA-mediated gene-silencing ability, but also reduce the toxic side effects of Dox, providing a valuable and safe approach for antitumor activity.

GO is another carbon nanomaterial that can also be used as a drug carrier for targeted therapy. Lu et al. reported an anticancer drug delivery system based on aptamer-functionalized GO by employing decitabine (DAC) and A549 cells as anticancer drugs and target cell models, respectively. Aptamer A1, which binds to A549 cells with high specificity and affinity, was attached to GO followed by loading DAC onto GO, leading to the formation of the A1-GO/DAC complex. The release of DAC from the complex in the target cell is pH-dependent, and DAC is released under acidic conditions (pH 5.5). The cell viability assay clearly demonstrated that the therapeutic efficacy of the complex for inhibiting the growth of cancer cells is much higher than that of the DAC-free drug, rendering this system promising for target therapy [228]. Alibolandi et al. designed an aptamer-decorated dextran (DEX)-coated nano-GO for targeted drug delivery. The DEX was covalently conjugated to the surface of nano-GO sheets, forming stable biocompatible dextran-coated GO (GO-DEX). AS1411 aptamer targeting nucleolin was introduced in GO-DEX by linking hydroxyl groups with DEX. GO-DEX-Apt was then

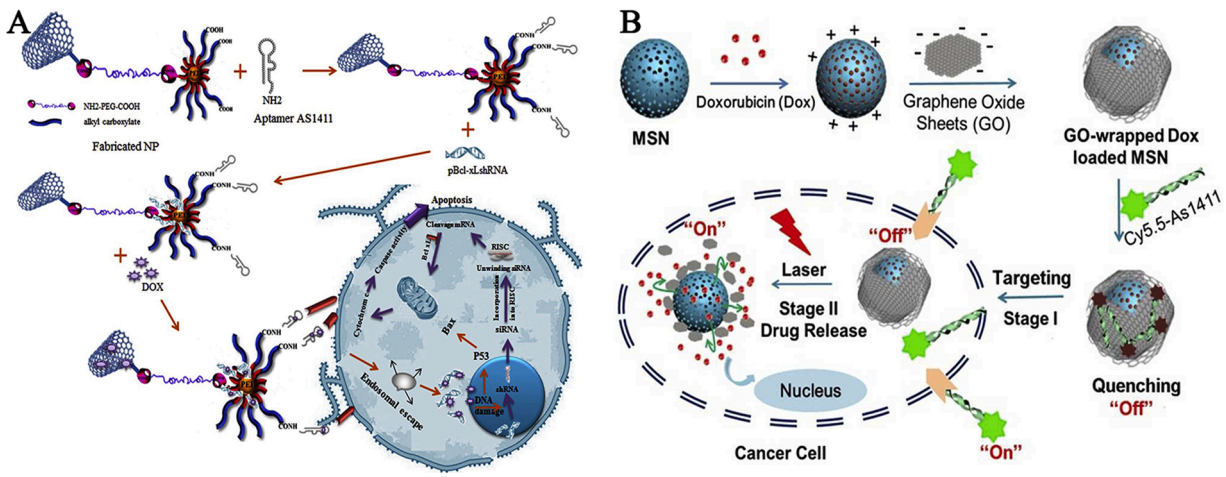

Fig. 17. Aptamer-SWNTs or GO-drugs conjugated system. (A) Schematic illustration of Bcl-xL shRNA and Dox co-delivery into gastric cancer cells using AS1411 aptamer-conjugated SWNTs. AS1411 aptamer was covalently linked to shRNA-SWNT-PEG-PEI conjugate followed by intercalation of Dox with pBcl-xL shRNA-SWCNT-PEG-PEI-Apt. In target cell, the synergistic effect of Bcl-xL shRNA and Dox could greatly enhance the therapeutic efficacy. Fig. 17A adapted from ref. [227]. (B) Schematic representation of Cy5.5-labeled AS1411 aptamer-targeting photoresponsive drug delivery system using GO-wrapped Dox-loaded MSN. The release of drug in the target cell was controlled by NIR light. The MSN-Dox@GO-Apt with two "off-on"switches were controlled by aptamer targeting and light triggering, respectively. Fig. 17B adapted from ref. [230].

used for loading curcumin (CUR) via π-stacking interaction, and the GO-DEX-Apt-CUR complex was formed. The complex could efficiently enter into nucleolin-overexpressed cancer cells, and displayed a greatly higher cytotoxicity toward these target cells, making this targeted nanoscale drug delivery vehicle promising for cancer chemotherapy [229]. Tang et al. developed a novel photoresponsive drug delivery system based on GO-wrapped mesoporous silica nanoparticles (MSN@GO) for light-mediated drug release and aptamer-targeted cancer therapy (Fig. 17B) [230]. Dox was first loaded by MSN, and then negatively charged GO nanosheets were wrapped around the surface of the positively charged MSN through electrostatic interactions. Afterwards, the Cy5.5-labeled AS1411 aptamer was attached to GO via π-π stacking, resulting in the quenching of the dye. After the uptake of the complex into the target cell, the fluorescence of Cy5.5 was restored. In the absence of laser irradiation, GO acted as a gatekeeper to prevent the loaded Dox from leaking. After laser irradiation, the photoresponsive drug delivery system is activated, causing the release of Dox. Importantly, the MSN-Dox@GO-Apt platform used for killing cancer cells could introduce the synergism of chemotherapy and photothermal therapy, which is much more effective than monotherapies, providing a new approach for cancer treatment.

Although these two carbon nanomaterials are good candidates for targeted delivery, their toxicity should be further considered [231,232]; the concentration, degree of functionalization, and physical form might all affect the toxicity of carbon nanomaterials [233,234]. In addition, the property of easily depolymerizing in vivo restricts their application in the biomedical field.

4.4.4. Liposomes

Owing to their size and their dually hydrophobic and hydrophilic characteristics, liposomes can not only load hydrophobic drugs in their lipid bilayer membranes, but also encapsulate the hydrophilic drugs in the aqueous core [235]. The liposome surface can be modified with different ligands, which could enhance the ability of targeting treatment, reduce the side effects of drugs, increase the drug effectiveness, extend the systemic circulation time of liposomes, and increase drug accumulation in the target cells or tissues [236]. Accordingly, liposomes can be developed as an ideal vehicle for drug delivery for disease treatment. Xing et al. developed AS1411 aptamer-functionalized liposomes as a drug delivery system for targeted anticancer chemotherapy (Fig. 18A) [237]. Dox was first doped in the aqueous core of the liposome, and then the AS1411 aptamer was conjugated to the liposome via the hydrophobic interaction between the lipid bilayer membranes and the cholesterol end on the aptamer. The Apt-Dox-Lip complex showed selective internalization and enhanced cytotoxicity to MCF-7 breast cancer cells and xenograft MCF-7 breast tumors in nude mice, suggesting that AS1411 aptamer-functionalized liposomes can specifically bind nucleolin overexpressed on the MCF-7 cell surface, and implement drug delivery with high selectivity. The above work only involved one type of aptamer linked to the liposome. Kim et al. designed a Dox-loaded liposome linked with two types of DNA aptamers targeting the surface marker transmembrane glycoprotein mucin 1 antigen (MUC1) on breast cancer cells and cell surface glycoprotein CD44 antigen (CD44) on their cancer stem cells (CSCs) (Fig. 18B) [238]. The authors have proven that the dual-aptamosome-Dox complex displayed considerably higher cytotoxicity to both CSCs and cancer cells than to liposomes lacking the aptamers. Therefore, this dual aptamer-labeled liposome system is a useful tool for combating breast cancer because of its efficiency in targeting breast cancer cells as well as their CSCs. To monitor the real-time dynamic process of drug transport and its action, Kim et al. developed an aptamer-coupled liposome loading of QDs and siRNAs for the theragnosis of triple-negative breast cancer (Fig. 18C) [239]. Hydrophobic QDs were included into lipid bilayers, and then siRNAs were incorporated into the aqueous core of the liposome. Finally, an aptamer targeting EGFR was attached to the QLs and formed aptamo-QLs. This complex not only provides fluorescence tumor images by QDs, but also inhibits tumor growth and metastasis via RNA interference. To enhance the efficiency of treatment and reduce the generation of drug resistance, Yu et al. constructed an aptamer-functionalized cationic liposome to co-deliver paclitaxel (PTX) and PLK1-targeted siRNA for the treatment of breast cancer (Fig. 18D) [240]. PTX was first encapsulated in the lipid bilayer membranes of liposomes (Lipo-PTX), and then siPLK1 was attached to the liposome followed by the conjugation of AS1411 aptamer onto Lipo-PTX-siPLK1. Using the AS1411/Lipo-PTX-siPLK1 delivery system, PTX and siPLK1 can be simultaneously transported into MCF-7 cells, which resulted in an increase in the number of apoptotic cells and reduced angiogenesis by the synergistic effect of these two therapeutic drugs. This platform was confirmed to be superior to the combined delivery of PTX and siRNA separately by different liposomal drug delivery systems. Hence, this delivery method based on the simultaneous delivery of chemotherapy drugs and siRNA may be useful for treating breast cancer in clinical

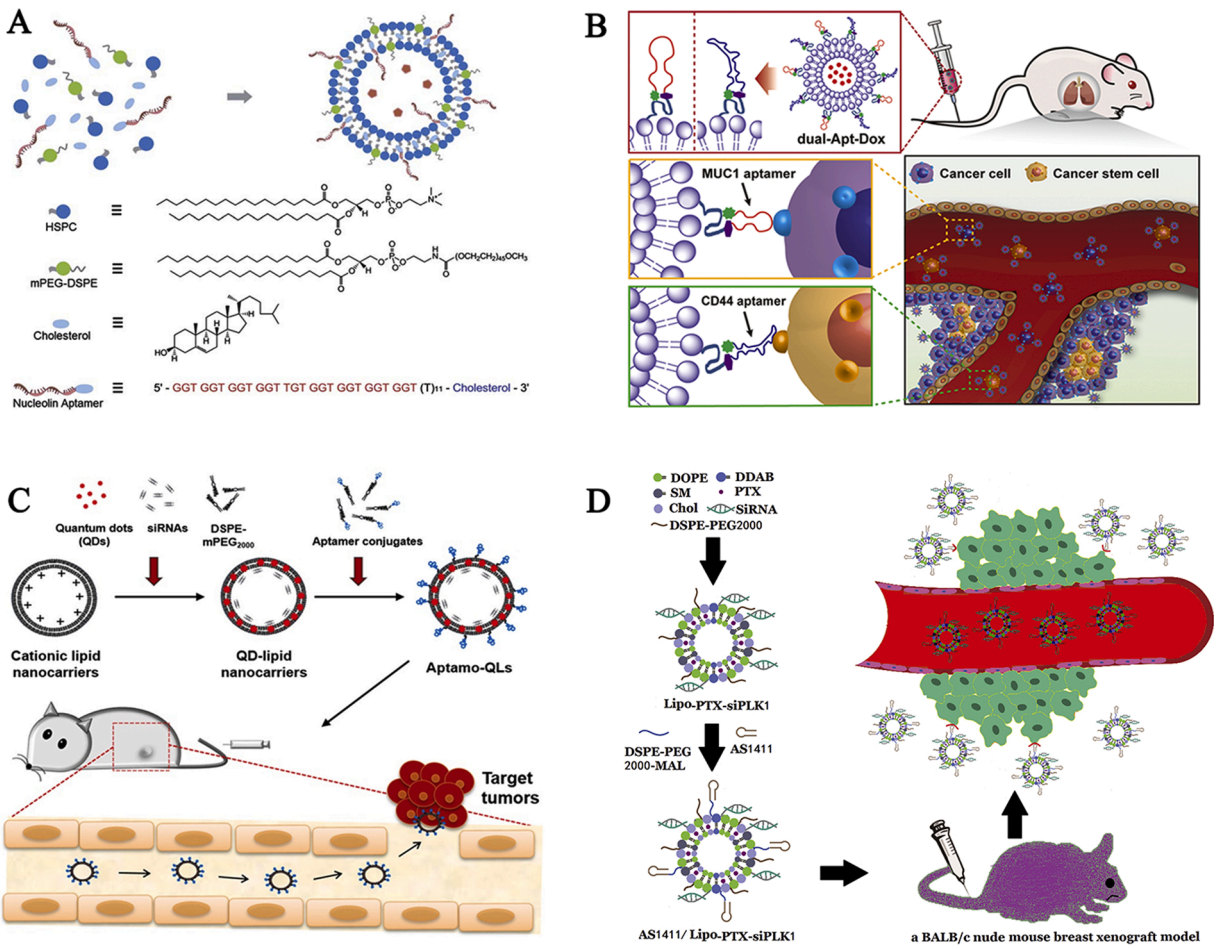

Fig. 18. Aptamer-Liposomes-drugs conjugated system. (A) Schematic illustration of nucleolin aptamer-functionalized liposome loading Dox for cancer therapy. Cholesterol-modified aptamers were immobilized onto the surface of liposome by intercalating the 3′cholesterol modification into the lipid bilayer. Fig. 18A adapted from ref. [237]; (B) Schematic illustration of dual-aptamer-conjugated liposomes loading Dox for cancer therapy. The MUC1 and CD44 DNA aptamers were conjugated separately with micelles through thiol and maleimide coupling reaction to form dual aptamer-conjugated micelles and subsequently mixed with Dox and plain liposomes for postinsertion. This conjugate showed cytotoxicity to both CSCs and cancer cells. Fig. 18B adapted from ref. [238]. Copyright (2019) American Chemical Society; (C) Schematic of the aptamer-based RNAi gene therapy and fluorescence tumor imaging. The aptamers targeting EGFR were conjugated to lipid nanocarriers loading QDs and siRNAs followed by intravenously administered. This conjugate extravasated through the leaky tumor vasculature and then targeted MDA-MB-231 tumors via specific recognition between the aptamer and EGFR. The QDs and siRNAs could provide fluorescence tumor images and inhibitory effects on tumor growth, respectively. Fig. 18C adapted from ref. [239]; (D) Schematic illustration of AS1411/Lipo-PTX-siPLK1 fabrication and its application in vivo therapy. The AS1411 aptamers were conjugated to liposomes encapsulating siRNAs and PTX to form AS1411/Lipo-PTX-siPLK1. The conjugate could simultaneously carry out chemotherapy and RNA interference in vivo. Fig. 18D adapted from ref. [240].

settings. It also provides a new idea for the treatment of other tumors. However, liposomes still have some drawbacks: lipid membranes are prone to oxidative hydrolysis, which increases the permeability of the bilayer membrane structure, leading to the leakage of the drugs. In addition, the hydrolysis of liposomes is also closely related to the pH, temperature, buffer solution and ionic strength. Thus, complex modifications are needed to overcome these defects during liposome preparation [241,242].

5. Conclusions and outlook

Aptamers, a recognition element that can bind to different types of targets with high affinity and specificity, have been widely used in diagnosis and therapy. In this review, we discuss the recent development of SELEX technology for aptamer selection and its applications for biosensors and targeted therapy. First, we summarized different types of SELEX technology that have emerged in recent years and been used for aptamer selection. The selection method, principle, and advantages and disadvantages were all concluded in the text. Second, several biosensors based on the strong binding affinity between aptamers and their target have been constructed. It is expected that these biosensors could assay their target with high selectivity and sensitivity based on different principles. Finally, we introduced three aptamer-based therapeutic strategies for disease therapy, including aptamer therapeutics, aptamer-drug conjugated systems, and aptamer-nanomaterial conjugated systems. These platforms could increase diagnosis accuracy and therapy efficiency, which provides the possibility of use in clinical practice.

Although great progress has been achieved in aptamer selection, aptasensor fabrication and nanomedicine technology development in recent years, some challenges should also be considered: 1) how to rapidly screen an aptamer with high affinity and specificity. The conventional SELEX procedure is simple, but time-consuming and labor-intensive. Emerging SELEX technologies can greatly reduce screening time and improve the affinities of aptamers; however, special equipment manipulated by skillful technicians is required. Hence, no standard SELEX methods have been established for aptamer screening. In addition, the conformation of aptamers is probably affected by physical and chemical factors, whereas the interaction between aptamers and targets is dependent on the conformation of aptamers. Accordingly, the aptamers obtained by in vitro SELEX might decrease their binding

ability to targets, leading to their practical applications being significantly limited. Future studies should focus on the construction of a screening model that is suitable for retaining the original binding conformation between aptamers and targets. 2) How to maintain the stability and specificity of aptasensors when they are used for assaying the target in a complex biological environment. Although many studies have been reported for target assays using aptamer-based biosensors, most of them were executed in the optimized buffer solution or in vitro culture. In fact, many aptamer-based biosensors may only display an optimal response under specific conditions. The detection efficiency decreases to some extent when these sensors are used in actual samples or in vivo experiments. Moreover, signal amplification caused by non-specific adsorption can be problematic in terms of the improvement of sensitivity. Therefore, we need to design adaptable aptasensors that will reserve their optimal functions under diverse conditions with high sensitivity and selectivity. 3) How to reduce the toxicity of nanomaterials used for in vivo applications, especially for non-degradable nanomaterials. Generally, nanomaterials used for loading aptamers or drugs exhibit toxicity toward target cells. Additionally, some nanomaterials can be enriched in the human body, causing many side effects, including inflammatory reactions, oxidative damage, and cell apoptosis. Even if some nanomaterials can be discharged from the body, they can cause irreversible damage to the environment. This critical issue remains to be fully investigated before entering clinical practice. To address this issue, future studies should concentrate on developing new surface modification technologies to enhance their biocompatibility while reducing toxicity, which can be beneficial for clinical applications.

Taken together, aptamers are appealing multifunctional tools that can be employed for the development of biosensors and targeted therapies. However, some major challenges must be overcome, and some critical issues still need to be resolved. Thus, the investigation and development of prospective diagnostic and therapeutic strategies will fuel the growth of the aptamer field in the future.

Declaration of Competing Interest

The authors declare that they do not have any commercial or associative interest that represents a conflict of interest in connection with the work submitted.

Acknowledgments

We would like to thank National Natural Science Foundation (81803964, 81774126, 82074250), China Postdoctoral Science Foundation (2018M630906, 2019T120707), Natural Science Foundation of Hunan Province (2020JJ4465, 2020JJ4063), Training Program for Outstanding Young Innovators of Changsha, Key Subjects of Hunan University of Chinese Medicine<pathogenic biology (NO. 1) and First-class Discipline Construction Project of Basic Medicine in 13th Five-Year Plan of Hunan University of Chinese Medicine (No. 6) for the financial support. We would like to thank Editage (www.editage.cn) for English language editing.

References

[1] A.D. Ellington, J.W. Szostak, In vitro selection of RNA molecules that bind specific ligands, Nature 346 (1990) 818–822.
[2] C. Tuerk, L. Gold, Systematic evolution of ligands by exponential enrichment: RNA ligands to bacteriophageT4 DNA polymerase, Science 249 (1990) 505–510.
[3] Y. Ning, W.K. Li, Y.F. Duan, M. Yang, L. Deng, High specific DNAzyme-aptamer sensor for *Salmonella paratyphi A* using single-walled nanotubes-based dual fluorescence-spectrophotometric methods, J. Biomol. Screen. 19 (2014) 1099–1106.
[4] H. Li, X.H. Ding, Z.H. Peng, L. Deng, Aptamer selection for the detection of *Escherichia coli* K88, Can. J. Microbiol. 57 (2011) 453–459.
[5] A. Sachan, M. Ilgu, A. Kempema, G.A. Kraus, M.N. Hamilton, Specificity and ligand affinities of the cocaine aptamer: impact of structural features and physiological NaCl, Anal. Chem. 88 (2016) 7715–7723.
[6] D.E. Huizenga, J.W. Szostak, A DNA aptamer that binds adenosine and Atp, Biochemistry 34 (1995) 656.
[7] H.P. Hofmann, S. Limmer, V. Hornung, M. Sprinzl, Ni^{2+}-binding RNA motifs with an asymmetric purine-rich internal loop and a G-A base pair, RNA 3 (1997) 1289–1300.
[8] L. Li, B. Li, Y. Qi, Y. Jin, Label-free aptamer-based colorimetric detection of mercury ions in aqueous media using unmodified gold nanoparticles as colorimetric probe, Anal. Bioanal. Chem. 8 (2009) 2051–2057.
[9] Y.F. Duan, Y. Ning, Y. Song, L. Deng, Fluorescent aptasensor for the determination of *Salmonella typhimurium* based on a graphene oxide platform, Microchim. Acta 181 (2014) 647–653.
[10] M. Yang, Z.H. Peng, Y. Ning, L. Deng, Highly specific and cost-efficient detection of *Salmonella paratyphi* A combining aptamers with single-walled carbon nanotubes, Sensors 13 (2013) 6865–6881.
[11] H. Feng, J. Beck, M. Nassal, K.H. Hu, A SELEX-screened aptamer of human hepatitis B virus RNA encapsidation signal suppresses viral replication, PLoS One 6 (2011), e27862.
[12] S.J. Kim, M.Y. Kim, J.H. Lee, J.C. You, S. Jeong, Selection and stabilization of the RNA aptamers against the human immunodefificiency virus type-1 nucleocapsid protein, Biochem. Biophys. Res. Commun. 291 (2002) 925–931.
[13] E. Kim, P. Dua, S. Kim, Cell-based aptamer selection for diagnosing cancer and predicting cancer progression, Toxicol. Environ. Health Sci. 1 (2009) 140–143.
[14] Z.W. Tang, D.H. Shangguan, K.M. Wang, H. Shi, K. Sefah, P. Mallikratchy, H. W. Chen, Y. Li, W.H. Tan, Selection of aptamers for molecular recognition and characterization of cancer cells, Anal. Chem. 79 (2007) 4900–4907.
[15] J. Liu, H.X. Liu, K. Sefah, B. Liu, Y. Pu, D.V. Simaey, W.H. Tan, Selection of aptamers specific for adipose tissue, PLoS One 7 (2012), e37789.
[16] J.Q. He, J.Y. Wang, N. Zhang, L.Y. Shen, L.L. Wang, X. Xiao, Y. Wang, T. Bing, X. J. Liu, S.Q. Li, D.H. Shangguan, In vitro selection of DNA aptamers recognizing drug-resistant ovarian cancer by cell-SELEX, Talanta 194 (2019) 437–445.
[17] J. Wang, T. Gao, Y. Luo, Z.L. Wang, Y.J. Zhang, Y. Zhang, Y.Y. Zhang, R.J. Pei, In vitro selection of a DNA aptamer by cell-SELEX as a molecular probe for cervical cancer recognition, J. Mol. Evol. 87 (2019) 72–82.
[18] Q.Y. Wu, N.Q. Lin, T. Tian, Z. Zhu, L. Wu, H.Y. Wang, D.L. Wang, D.Z. Kang, R. J. Tian, C.Y. Yang, Evolution of nucleic acid aptamers capable of specifically targeting glioma stem cells via cell-SELEX, Anal. Chem. 91 (2019) 8070–8077.
[19] K. Han, Z. Liang, N. Zhou, Design strategies for aptamer-based biosensors, Sensors 10 (2010) 541–4557.
[20] S.D. Jayasena, Aptamers: an emerging class of molecules that rival antibodies in diagnostics, Clin. Chem. 45 (1999) 1628–1650.
[21] C.S. Ferreira, S. Missailidis, Aptamer-based therapeutics and their potential in radiopharmaceutical design, Braz. Arch. Biol. Technol. 50 (2007) 63–76.
[22] Y. Wang, Z.H. Li, D.H. Hu, C.T. Lin, J.H. Li, Y.H. Lin, Aptamer/graphene oxide nanocomplex for in situ molecular probing in living cells, J. Am. Chem. Soc. 132 (2010) 9274–9276.
[23] H.X. Tan, L. Ma, T. Guo, H.Y. Zhou, L. Chen, Y.H. Zhang, H.J. Dai, Y. Yu, A novel fluorescence aptasensor based on mesoporous silica nanoparticles for selective and sensitive detection of aflatoxin B1, Anal. Chim. Acta 1068 (2019) 87–95.
[24] X. Weng, S. Neethirajan, A microfluidic biosensor using graphene oxide and aptamer-functionalized quantum dots for peanut allergen detection, Biosens. Bioelectron. 85 (2016) 649–656.
[25] The Eyetech Study Group, Anti-vascular endothelial growth factor therapy for subfoveal choroidal neovascularization secondary to age-related macular degeneration: phase II study results, Ophthalmology 110 (2003) 979–986.
[26] M. Mascini, Aptamers and their applications, Anal. Bioanal. Chem. 390 (2008) 987–988.
[27] N.D. Le, M. Yazdani, V.M. Rotello, Array-based sensing using nanoparticles: an alternative approach for cancer diagnostics, Nanomedicine 9 (2014) 1487–1498.
[28] M. Platt, W. Rowe, D.C. Wedge, D.B. Kell, J. Knowles, P.J.R. Day, Aptamer evolution for array-based diagnostics, Anal. Biochem. 390 (2009) 203–205.
[29] V.D. Franciscis, A theranostic' SMART' aptamer for targeted therapy of prostate cancer, Mol. Ther. 22 (2014) 1886–1888.
[30] V. Cereda, V. Formica, G. Massimiani, L. Tosetto, M. Roselli, Targeting metastatic castration-resistant prostate cancer: mechanisms of progression and novel early therapeutic approaches, Expert Opin. Investig. Drugs 23 (2014) 469–487.
[31] X.F. Huang, J.M. Zhong, J. Ren, D.D. Wen, W.W. Zhao, Y. Huan, A DNA aptamer recognizing MMP14 for in vivo and in vitro imaging identified by cell SELEX, Oncol. Lett. 18 (2019) 265–274.
[32] J. Charlton, J. Sennello, D. Smith, In vivo imaging of inflammation using an aptamer inhibitor of human neutrophil elastase, Chem. Biol. 4 (1997) 809–816.
[33] H.J. Zhang, X. Zhao, L.J. Chen, C.X. Yang, X.P. Yan, Dendrimer grafted persistent luminescent nanoplatform for aptamer guided tumor imaging and acid-responsive drug delivery, Talanta 219 (2020), 121209.
[34] L.Y. Wan, W.F. Yuan, W.B. Ai, Y.W. Ai, J.J. Wang, L.Y. Chu, Y.Q. Zhang, J.F. Wu, An exploration of aptamer internalization mechanisms and their applications in drug delivery, Expert Opin. Drug Deliv. 16 (2019) 207–218.
[35] Q. Zhao, M.H. Wu, X.C. Le, X.F. Li, Applications of aptamer affinity chromatography, TrAC Trend. Anal. Chem. 41 (2012) 46–57.
[36] T.S. Romig, C. Bell, D.W. Drolet, Aptamer affinity chromatography: combinatorial chemistry applied to protein purification, J. Chromatogr. B 731 (1999) 275–284.
[37] Z. Jiao, H.F. Zhang, S.H. Jiao, Z.N. Guo, D. Zhu, X.F. Zhao, A turn-on biosensor based aptamer-mediated carbon quantum dots nanoaggregate for acetamiprid detection in complex samples, Food Anal. Methods 12 (2019) 668–676.
[38] L. Zhang, P. Cui, B.C. Zhang, F. Gao, Aptamer-based turn-on detection of thrombin in biological fluids based on efficient phosphorescence energy transfer

from Mn-doped ZnS quantum dots to carbon nanodots, Chem. Eur. J. 19 (2013) 9242–9250.
[39] Y. Xiong, Y. Cheng, L. Wang, Y. Li, An "off-on'' phosphorescent aptasensor switch for the detection of ATP, Talanta 190 (2018) 226–234.
[40] D.Q. Lu, L. He, G. Zhang, A.P. Lv, R.W. Wang, X.B. Zhang, W.H. Tan, Aptamer-assembled nanomaterials for fluorescent sensing and imaging, Nanophotonics 6 (2017) 109–121.
[41] M.V. Berezovski, M. Lechmann, M.U. Musheev, T.W. Mak, S.N. Krylov, Aptamer-facilitated biomarker discovery (AptaBiD), J. Am. Chem. Soc. 130 (2009) 9137–9143.
[42] L.T. Cherney, N.M. Obrecht, S.N. Krylov, Theoretical modeling of masking dna application in aptamer-facilitated biomarker discovery, Anal. Chem. 85 (2013) 4157–4164.
[43] T.J. Wang, J. Ray, Atamper-based molecular imaging, Protein Cell 3 (2012) 739–754.
[44] D.H.J. Bunka, P.G. Stockley, Aptamers come of age - at last, Nat. Rev. Microbiol. 4 (2006) 588–596.
[45] M. Citartan, E.S. Ch'ng, T.S. Rozhdestvensky, T.H. Tang, Aptamers as the 'capturing'agents in aptamer-based capture assays, Microchem. J. 128 (2016) 187–197.
[46] S.E. Osborne, A.D. Ellington, Nucleic acid selection and the challenge of combinatorial chemistry, Chem. Rev. 97 (1997) 349–370.
[47] W.H. Zhu, Z.J. Li, X.X. Liu, L. Deng, Determination of *Shigella flexneri* by a novel fluorescent aptasensor, Anal. Lett. 48 (2015) 2870–2881.
[48] X.R. Feng, K.Y. Liu, Y. Ning, L.J. Cheng, L. Deng, A label-free aptasensor for rapid detection of H1N1 virus based on graphene oxide and polymerase-aided signal amplification, J. Nanomed. Nanotechnol. 6 (2015) 288.
[49] C. Tuerk, S. MacDougal, L. Gold, RNA pseudoknots that inhibit human immunodeficiency virus type 1 reverse transcriptase, Proc. Natl. Acad. Sci. U. S. A. 89 (1992) 6988–6992.
[50] T.W. Wiegand, B.P. Williams, S.C. Dreskin, M. Jouvin, J. Kinet, D. Tasset, High-affinity oligonucleotide ligands to human IgE inhibit binding to Fc epsilon receptor I, J. Immunol. 157 (1996) 221–230.
[51] J. Ruckman, L.S. Green, J. Beeson, S. Waugh, W.L. Gillette, D.D. Henninger, L. Claesson-Welsh, N. Janjić, 2'-Fluoropyrimidine RNA-based aptamers to the 165-amino acid form of vascular endothelial growth factor (VEGF165). Inhibition of receptor binding and VEGF-induced vascular permeability through interactions requiring the exon 7-encoded domain, J. Biol. Chem. 273 (1998) 2056–20567.
[52] S. Sekiya, K. Noda, F. Nishikawa, T. Yokoyama, P.K.R. Kumar, S. Nishikawa, Characterization and application of a novel RNA aptamer against the mouse prion protein, J. Biochem. 139 (2006) 383–390.
[53] J.R. Hesselberth, D. Miller, J. Robertus, A.D. Ellington, In vitro selection of RNA molecules that inhibit the activity of ricin A-chain, J. Biol. Chem. 275 (2000) 4937–4942.
[54] S.C. Gopinath, Methods developed for SELEX, Anal. Bioanal. Chem. 387 (2007) 171–182.
[55] S. Tombelli, M. Minunni, M. Mascini, Analytical applications of aptamers, Biosens. Bioelectron. 20 (2005) 2424–2434.
[56] K.M. Song, M. Cho, H. Jo, K. Min, S.H. Jeon, T. Kim, M.S. Han, J.K. Ku, C. Ban, Gold nanoparticle-based colorimetric detection of kanamycin using a DNA aptamer, Anal. Biochem. 415 (2011) 175–181.
[57] D. Lévesque, J.D. Beaudoin, S. Roy, J.P. Perreault, In vitro selection and characterization of RNA aptamers binding thyroxine hormone, Biochem. J. 403 (2007) 129–138.
[58] E. Vianini, M. Palumbo, B. Gatto, In vitro selection of DNA aptamers that bind L-tyrosinamide, Bioorg. Med. Chem. 9 (2001) 2543–2548.
[59] J.C. Cox, A.D. Ellington, Automated selection of anti-protein aptamers, Bioorg. Med. Chem. 9 (2001) 2525–2531.
[60] J.G. Bruno, J.L. Kiel, Use of magnetic beads in selection and detection of biotoxin aptamers by electrochemiluminescence and enzymatic methods, Biotechniques 32 (2002) 178–180.
[61] S. Weiss, D. Proske, M. Neumann, M.H. Groschup, H.A. Kretzschmar, M. Famulok, E. Winnacker, RNA aptamers specifically interact with the prion protein PrP, J. Virol. 71 (1997) 8790–8797.
[62] K.F. Bryant, J.C. Cox, H. Wang, J.M. Hogle, A.D. Ellington, D.M. Coen, Binding of herpes simplex virus-1 US11 to specific RNA sequences, Nucleic Acids Res. 33 (2005) 6090–6100.
[63] R. Stoltenburg, C. Reinemann, B. Strehlitz, FluMag-SELEX as an advantageous method for DNA aptamer selection, Anal. Bioanal. Chem. 383 (2005) 83–91.
[64] Y.S. Kim, C.J. Hyun, I.A. Kim, M.B. Gu, Isolation and characterization of enantioselective DNA aptamers for ibuprofen, Bioorg. Med. Chem. 18 (2010) 3467–3473.
[65] S. Xu, H. Yuan, S. Chen, A. Xu, J. Wang, L. Wu, Selection of DNA aptamers against polychlorinated biphenyls as potential biorecognition elements for environmental analysis, Anal. Biochem. 423 (2012) 195–201.
[66] Z.H. Peng, M. Ling, Y. Ning, L. Deng, Rapid fluorescent detection of Escherichia coli K88 based on DNA aptamer library as direct and specific reporter combined with immuno-magnetic separation, J. Fluoresc. 24 (2014) 1159–1168.
[67] R.K. Mosing, M.T. Bowser, Isolating aptamers using capillary electrophoresis-SELEX (CE-SELEX), Methods Mol. Biol. 535 (2009) 33–43.
[68] Z. Xi, R. Huang, Y. Deng, N.Y. He, Progress in selection and biomedical applications of aptamers, J. Biomed. Nanotechnol. 10 (2014) 3043–3062.
[69] N.S. Hamedani, J. Muller, Capillary electrophoresis for the selection of DNA aptamers recognizing activated protein C, Methods Mol. Biol. 1380 (2016) 61–75.
[70] J.H. Yan, H.J. Xiong, S.D. Cai, N.C. Wen, Q.Y. He, Y.F. Liu, D.M. Peng, Z.B. Liu, Advances in aptamer screening technologies, Talanta 200 (2019) 124–144.
[71] L. Dong, Q. Tan, W. Ye, D. Liu, H. Chen, H. Hu, D. Wen, Y. Liu, Y. Cao, J. Kang, J. Fan, W. Guo, W. Wu, Screening and identifying a novel ssDNA aptamer against alpha-fetoprotein using CE-SELEX, Sci. Rep. 5 (2015) 15552.
[72] S.D. Mendonsa, M.T. Bowser, In vitro selection of aptamers with affinity for neuropeptide Y using capillary electrophoresis, J. Am. Chem. Soc. 127 (2005) 9382–9383.
[73] S.D. Mendonsa, M.T. Bowser, In vitro selection of high-affinity DNA ligands for human IgE using capillary electrophoresis, Anal. Chem. 76 (2004) 5387–5392.
[74] R.M. Eaton, J.A. Shallcross, L.E. Mael, K.S. Mears, L. Minkoff, D.J. Scoville, R. J. Whelan, Selection of DNA aptamers for ovarian cancer biomarker HE4 using CE-SELEX and high-throughput sequencing, Anal. Bioanal. Chem. 407 (2015) 6965–6973.
[75] M.V. Berezovski, S.N. Krylov, Nonequilibrium capillary electrophoresis of equilibrium mixtures—a single experiment reveals equilibrium and kinetic parameters of protein-DNA interactions, J. Am. Chem. Soc. 124 (2002) 13674–13675.
[76] S.D. Mendonsa, M.T. Bowser, In vitro evolution of functional DNA using capillary electrophoresis, J. Am. Chem. Soc. 126 (2004) 20–21.
[77] M. Jing, M.T. Bowser, Isolation of DNA aptamers using micro free flow electrophoresis, Lab Chip (2011) 3703–3709.
[78] L. Hung, C. Wang, Y. Che, C. Fu, H. Chang, K. Wang, G. Lee, Screening of aptamers specific to colorectal cancer cells and stem cells by utilizing on-chip cell-SELEX, Sci. Rep. 5 (2015) 10326.
[79] C.H. Weng, C.J. Huang, G.B. Lee, Screening of aptamers on microfluidic systems for clinical applications, Sensors 12 (2012) 9514–9529.
[80] X.H. Lou, J.R. Qian, Y. Xiao, L. Viel, A.E. Gerdon, E.T. Lagally, P. Atzberger, T. M. Tarasow, A.J. Heeger, H.T. Soh, Micromagnetic selection of aptamers in microfluidic channels, Proc. Natl. Acad. Sci. U. S. A. 106 (2009) 2989–2994.
[81] J.R. Qian, X.H. Lou, Y.T. Zhang, Y. Xiao, H.T. Soh, Generation of highly specific aptamers via micromagnetic selection, Anal. Chem. 81 (2009) 5490–5495.
[82] L. Peng, B.J. Stephens, K. Bonin, R. Cubicciotti, M. Guthold, A combined atomic Force/Fluorescence microscopy technique to select aptamers in a single cycle from a small pool of random oligonucleotides, Microsc. Res. Techniq. 70 (2007) 372–381.
[83] K.A. Dittmar, P. Jiang, J.W. Park, K. Amirikian, J. Wan, S. Shen, Y. Xing, R. P. Carstens, Genome-wide determination of a broad ESRP-regulated posttranscriptional network by high-throughput sequencing, Mol. Cell. Biol. 32 (2012) 1468–1482.
[84] M.A. Ditzler, M.J. Lange, D. Bose, C.A. Bottoms, K.F. Virkler, A.W. Sawyer, A. S. Whatley, W. Spollen, S.A. Givan, D.H. Burke, High-throughput sequence analysis reveals structural diversity and improved potency among RNA inhibitors of HIV reverse transcriptase, Nucleic Acids Res. 41 (2013) 1873–1884.
[85] V.T. Nguyen, Y.S. Kwon, J.H. Kim, M.B. Gu, Multiple GO-SELEX for efficient screening of flexible aptamers, Chem. Commun. 50 (2014) 10513–10516.
[86] S. Wu, N. Duan, W.X. Zhang, S. Zhao, Z.P. Wang, Screening and development of DNA aptamers as capture probes for colorimetric detection of patulin, Anal. Biochem. 508 (2016) 58–64.
[87] Y.Y. Koh, M. Wickens, Determining the RNA specificity and targets of RNA-binding proteins using a three-hybrid system, Methods Enzymol 539 (2014) 163–181.
[88] K.B. Jensen, B.L. Atkinson, M.C. Willis, T.H. Koch, L. Gold, Using in vitro selection to direct the covalent attachment of human immunodeficiency virus type 1 Rev protein to high-affinity RNA ligands, Proc. Natl. Acad. Sci. U. S. A. 92 (1995) 12220–12224.
[89] M. Blank, T. Weinschenk, M. Priemer, H. Schluesener, Systematic evolution of a DNA aptamer binding to rat brain tumor microvessels, J. Biol. Chem. 276 (2001) 16464–16468.
[90] X. Yang, X. Li, T.W. Prow, L.M. Reece, S.E. Bassett, B.A. Luxon, N.K. Herzog, J. Aronson, R.E. Shope, J.F. Leary, D.G. Gonestein, Immunofluorescence assay and flow-cytometry selection of bead-bound aptamers, Nucleic Acids Res. 31 (2003) e54.
[91] M. Khati, M. Schuman, J. Ibrahim, Q. Sattentau, S. Gordon, W. James, Neutralization of infectivity of diverse R5 clinical isolates of human immunodeficiency virus type 1 by gp120-binding 2′F-RNA aptamers, J. Virol. 77 (2003) 12692–12698.
[92] P.S. Katsamba, D.G. Myszka, I.A. Laird-Offringa, Two functionally distinct steps mediate high affinity binding of U1A protein to U1 hairpin II RNA, J. Biol. Chem. 276 (2001) 21476–21481.
[93] O.S. Wolfbeis, Fiber-optic chemical sensors and biosensors, Anal. Chem. 74 (2002) 2663–2677.
[94] J. Wang, Electroanalysis and biosensors, Anal. Chem. 71 (1999) 328–332.
[95] L.Y. Jiang, X.X. Hang, P. Zhang, J.T. Zhang, Y.F. Wang, W. Wang, L.J. Ren, A highly sensitive fluorescence-enhanced aptasensor based on polyAn-aptamer nanostructure, Microchem. J. 148 (2019) 285–290.
[96] M.A. Abedalwafa, Z. Tang, Y. Qiao, Q. Mei, L. Wang, An aptasensor strip-based colorimetric determination methodfor kanamycin using cellulose acetate nanofibers decorated dna-gold nanoparticle bioconjugates, Microchim. Acta 187 (2020) 360.
[97] A. Sharma, J. Bhardwaj, J. Jang, Label-free, highly sensitive electrochemical aptasensors using polymer-modified reduced graphene oxide for cardiac biomarker detection, ACS Omega 5 (2020) 3924–3931.
[98] Y. Yao, H. Wang, X. Wang, X. Wang, F. Li, Development of a chemiluminescent aptasensor for ultrasensitive and selective detection of aflatoxin b1 in peanut and milk, Talanta 201 (2019) 52–57.

[99] V.I. Kukushkin, N.M. Ivanov, A.A. Novoseltseva, A.S. Gambaryan, I.V. Yaminsky, A.M. Kopylov, E.G. Zavyalova, Highly sensitive detection of influenza virus with SERS aptasensor, PLoS One 14 (2019), e0216247.
[100] W.J. Wang, C.L. Chen, M.X. Qian, X.S. Zhao, Aptamer biosensor for protein detection based on guanine-quenching, Sens. Actuators B-Chem. 129 (2008) 211–217.
[101] L. Dong, C.J. Hou, H.B. Fa, M. Yang, H.X. Wu, L. Zhang, D.Q. Huo, Highly sensitive fluorescent sensor for cartap based on fluorescence resonance energy transfer between gold nanoparticles and rhodamine B, J. Nanosci. Nanotechnol. 18 (2018) 2441–2449.
[102] K. Shao, L. Wang, Y. Wen, T. Wang, Y. Teng, Z. Shen, Z. Pan, Near-infrared carbon dots-based fluorescence turn on aptasensor for determination of carcinoembryonic antigen in pleural effusion, Anal. Chim. Acta 1068 (2019) 52–59.
[103] J.Y. Tian, W.Q. Wei, J.W. Wang, S.J. Ji, G.C. Chen, J. Lu, Fluorescence resonance energy transfer aptasensor between nanoceria and graphene quantum dots for the determination of ochratoxin A, Anal. Chim. Acta 1000 (2018) 265–272.
[104] S.K. Arya, P. Zhurauski, P. Jolly, M.R. Batistuti, M. Mulato, P. Estrela, Capacitive aptasensor based on interdigitated electrode for breast cancer detection in undiluted human serum, Biosens. Bioelectron. 102 (2017) 106–112.
[105] Y. Xiao, A.A. Lubin, A.J. Heeger, K.W. Plaxco, Label-free electronic detection of thrombin in blood serum by using an aptamer-based sensor, Angew. Chem. Int. Ed. 44 (2005) 5456–5459.
[106] X. Zuo, S. Song, J. Zhang, D. Pan, L. Wang, C. Fan, A target-responsive electrochemical aptamer switch (treas) for reagentless detection of nanomolar ATP, J. Am.Chem. Soc. 129 (2007) 1042–1043.
[107] J.W. Liu, Y. Lu, Non-base pairing DNA provides a new dimension for controlling aptamer-linked nanoparticles and sensors, J. Am.Chem. Soc. 129 (2007) 8634–8643.
[108] O.A. Alsager, K.M. Alotaibi, A.M. Alswieleh, B.J. Alyamani, Colorimetric aptasensor of vitamin D3: a novel approach to eliminate residual adhesion between aptamers and gold nanoparticles, Sci. Rep. 8 (2018) 12947.
[109] S. Wang, W. Li, K.K. Chang, J. Liu, Q.Q. Guo, H.F. Sun, M. Jiang, H. Zhang, J. Chen, J.D. Hu, Localized surface plasmon resonance-based abscisic acid biosensor using aptamer-functionalized gold nanoparticles, PLoS One 12 (2017), e0185530.
[110] Y.S. Borghei, M. Hosseini, M. Dadmehr, S. Hosseinkhani, M.R. Ganjali, R. Sheikhnejad, Visual detection of cancer cells by colorimetric aptasensor based on aggregation of gold nanoparticle induced by DNA hybridization, Anal. Chim. Acta 904 (2016) 92–97.
[111] K. Abnous, N.M. Danesh, M. Ramezani, A.S. Emrani, S.M. Taghdisi, A novel colorimetric sandwich aptasensor based on an indirect competitive enzyme-free method for ultrasensitive detection of chloramphenicol, Biosens. Bioelectron. 78 (2016) 80–86.
[112] X. Ma, L. Song, N. Zhou, Y. Xia, Z. Wang, A novel aptasensor for the colorimetric detection of *s. typhimurium* based on gold nanoparticles, Int. J. Food Microbiol. 245 (2017) 1–5.
[113] J.G. Bruno, A.M. Richarte, M.P. Carrillo, A. Edge, An aptamer beacon responsive to botulinum toxins, Biosens. Bioelectron. 31 (2012) 240–243.
[114] N. Tuleuova, A. Revzin, Micropatterning of aptamer beacons to create cytokine-sensing surfaces, Cell. Mol. Bioeng. 3 (2010) 337–344.
[115] S.M. Sanzani, M. Reverberi, C. Fanelli, A. Ippolito, Detection of ochratoxin a using molecular beacons and real-time PCR thermal cycler, Toxins (Basel) 7 (2015) 812–820.
[116] C.W. Chi, Y.H. Lao, Y.S. Li, L.C. Chen, A quantum dot-aptamer beacon using a DNA intercalating dye as the FRET reporter: application to label-free thrombin detection, Biosens. Bioelectron. 26 (2011) 3346–3352.
[117] B. Hall, S. Cater, M. Levy, A.D. Ellington, Kinetic optimization of a protein-responsive aptamer beacon, Biotechnol. Bioeng. 103 (2009) 1049–1059.
[118] J.Q. Zhang, Y.S. Wang, J.H. Xue, H.X. Yang, J. Liang, L.F. Shi, X.L. Xiao, A gold nanoparticles-modified aptamer beacon for urinary adenosine detection based on structure-switching/fluorescence-"turning on" mechanism, J. Pharmaceut. Biomed. 70 (2012) 362–368.
[119] F. Zhang, S.M. Li, K. Cao, P.J. Wang, Y. Su, X.H. Zhu, Y. Wan, A microfluidic love-wave biosensing device for PSA detection based on an aptamer beacon probe, Sensors 15 (2015) 13839–13850.
[120] S. Nasseri, S. Ebrahimi, M. Abtahi, R. Saeedi, Synthesis and characterization of polysulfone/graphene oxide nano-composite membranes for removal of bisphenol A from water, J. Environ. Manage. 205 (2017) 174–182.
[121] Y. Zhang, M. Zhang, H. Jiang, J. Shi, F. Li, Y. Xia, G. Zhang, H. Li, Bio-inspired layered chitosan/graphene oxide nanocomposite hydrogels with high strength and pH-driven shape memory effect, Carbohydr. Polym. 177 (2017) 116–125.
[122] H. Lv, S. Li, Y.M. Liu, G.K. Wang, X. Li, Y. Lu, J.J. Wang, A reversible fluorescent INHIBIT logic gate for determination of silver and iodide based on the use of graphene oxide and a silver-selective probe DNA, Microchim. Acta 182 (2015) 2513–2520.
[123] Y. Ning, Q. Gao, Q.X. Zhang, K. Wei, L.L. Chen, A graphene oxide–based sensing platform for the determination of methicillin-resistant *Staphylococcus aureus* based on strand-displacement polymerization recycling and synchronous fluorescent signal amplification, J. Biomol. Screen. 21 (2016) 851–857.
[124] L.J. Wang, J.N. Tian, Y. Huang, X.W. Lin, W. Yang, Y.C. Zhao, S.L. Zhao, Homogenous fluorescence polarization assay for the DNA of HIV A T7 by exploiting exonuclease-assisted quadratic recycling amplification and the strong interaction between graphene oxide and ssDNA, Microchim. Acta 183 (2016) 2147–2153.
[125] X. Hu, Y. Liu, X. Qu, Q. Sun, A quantum dot-labelled aptamer/graphene oxide system for the construction of a half-adder and half-subtractor with high resettability, Chem. Commun. 53 (2017) 11181–11184.
[126] C.H. Lu, C.L. Zhu, J. Li, J.J. Liu, X. Chen, H.H. Yang, Using graphene to protect DNA from cleavage during cellular delivery, Chem. Commun. 46 (2010) 3116–3118.
[127] Y. Wang, Z. Li, T.J. Weber, D. Hu, C.T. Lin, J. Li, Y. Lin, In situ live cell sensing of multiple nucleotides exploiting DNA/RNA aptamers and graphene oxide nanosheets, Anal. Chem. 85 (2013) 6775–6782.
[128] J.X. Tan, F.Y. Wang, Z.F. Wang, Q.J. Lu, L. Deng, An enzyme-free fluorometric nanoprobe for chloramphenicol based on signal amplification using graphene oxide sheets, Microchim. Acta 187 (2020) 319.
[129] K. Hu, H. Yang, J. Zhou, S. Zhao, J. Tian, Aptasensor for amplified IgE sensing based on fluorescence quenching by graphene oxide, Luminescence 28 (2013) 662–666.
[130] M. Joo, S.H. Baek, S.A. Cheon, H.S. Chun, S.W. Choi, T.J. Park, Development of aflatoxin B-1 aptasensor based on wide-range fluorescence detection using graphene oxide quencher, Colloids Surf. B Biointerfaces 154 (2017) 27–32.
[131] J.F. Liang, R. Wei, S. He, Y.K. Liu, L. Guo, L.D. Li, A highly sensitive and selective aptasensor based on graphene oxide fluorescence resonance energy transfer for the rapid determination of oncoprotein PDGF-BB, Analyst 138 (2013) 1726–1732.
[132] X. Yan, W.K. Li, K.Y. Liu, L. Deng, Highly sensitive fluorescent aptasensor for *Salmonella paratyphi A* via DNase I-mediated cyclic signal amplification, Anal. Methods 7 (2015) 10243–10245.
[133] Y. Ning, Y.F. Duan, Y.Y. Feng, L. Deng, Label-free fluorescent aptasensor based on a graphene oxide self-assembled probe for the determination of of adenosine triphosphate, Anal. Lett. 47 (2014) 2350–2360.
[134] M.M. Yan, W.H. Bai, C. Zhu, Y.F. Huang, J. Yan, A.L. Chen, Design of nuclease-based target recycling signal amplification in aptasensors, Biosens. Bioelectron. 77 (2016) 613–623.
[135] K.Y. Liu, X. Yan, B.Y. Mao, S. Wang, L. Deng, Aptamer-based detection of Salmonella enteritidis using double signal amplification by Klenow fragment and dual fluorescence, Microchim. Acta 183 (2016) 643–649.
[136] L. Peng, Z. Zhu, Y. Chen, D. Han, W.H. Tan, An exonuclease III and graphene oxide-aided assay for DNA detection, Biosens. Bioelectron. 35 (2013) 475–478.
[137] J.K. Wang, T.X. Li, X.Y. Gao, Z.H. Lu, Exonuclease III protection assay with FRET probe for detecting DNA-binding proteins, Nucleic Acids Res. 33 (2005) e23.
[138] Y. Ning, L. Zou, Q. Gao, J. Hu, F.G. Lu, Graphene oxide-based fluorometric determination of methicillin-resistant *Staphylococcus aureus* by using target-triggered chain reaction and deoxyribonuclease-assisted recycling, Microchim. Acta. 185 (2018) 183.
[139] X. Li, X.L. Ding, J. Fan, Nicking endonuclease-assisted signal amplification of split molecular aptamer beacon for biomolecules detection using graphene oxide as sensing platform, Analyst 140 (2015) 7918–7925.
[140] Q. Li, Y.D. Wang, G.L. Shen, H. Tang, R.Q. Yu, J.H. Jiang, Split aptamer mediated endonuclease amplification for small-molecule detection, Chem. Commun. 51 (2015) 4196–4199.
[141] Y. Ning, K. Wei, L.J. Cheng, J. Hu, Q. Xiang, Fluorometric aptamer based determination of adenosine triphosphate based on deoxyribonuclease I-aided target recycling and signal amplification using graphene oxide as a quencher, Microchim. Acta 184 (2017) 1847–1854.
[142] X.Y. Lin, L. Cui, Y.S. Huang, Y. Lin, Y. Xie, Z. Zhu, B.C. Yin, X. Chen, C.Y.J. Yang, Carbon nanoparticle-protected aptamers for highly sensitive and selective detection of biomolecules based on nuclease-assisted target recycling signal amplification, Chem. Commun. 50 (2014) 7646–7648.
[143] U. Khan, I.O. Conner, Y.K. Gun'ko, J.N. Coleman, The preparation of hybrid films of carbon nanotubes and nano-graphite/graphene with excellent mechanical and electrical properties, Carbon 48 (2010) 2825–2830.
[144] M. Li, A nano-graphite/paraffin phase change material with high thermal conductivity, Appl. Energy 106 (2013) 25–30.
[145] Y. Wei, B.M. Li, X. Wang, Y.X. Duan, Magnified fluorescence detection of silver(I) ion in aqueous solutions by using nano-graphite-DNA hybrid and DNase I, Biosens. Bioelectron. 58 (2014) 276–281.
[146] J. Zhang, F.Y. Ran, W.B. Zhou, B. Shang, F. Yu, L. Wu, W.B. Hu, X.Q. He, Q. H. Chen, Ultrasensitive fluorescent aptasensor for MUC1 detection based on deoxyribonuclease I-aided target recycling signal amplification, RSC Adv. 8 (2018) 32009–32015.
[147] Y. He, F.Y. Tian, J. Zhou, B. Jiao, A fluorescent aptasensor for ochratoxin A detection based on enzymatically generated copper nanoparticles with a polythymine scaffold, Microchim. Acta 186 (2019) 199.
[148] Q. He, H. Luo, L. Tang, J. Liu, K. Chen, Q. Zhang, Y. Ning, Nanographite-based enhanced fluorescent biosensing of *Salmonella enteritidis* by applying deoxyribonuclease-assisted recycling, Microchim. Acta 184 (2017) 3875–3882.
[149] M. Lin, Z.H. Peng, L.J. Cheng, L. Deng, Rapid fluorescent detection of enterotoxigenic *Escherichia coli* (ETEC) K88 based on graphene oxide-dependent nanoquencher and Klenow fragment-triggered target cyclic amplification, Appl. Spectrosc. 69 (2015) 1175–1181.
[150] J.L. He, Y.F. Yang, G.L. Shen, R.Q. Yu, Electrochemical aptameric sensor based on the Klenow fragment polymerase reaction for cocaine detection, Biosens. Bioelectron. 26 (2011) 4222–4226.
[151] T.X. Yu, J.B. Li, Q.F. Liu, W. Cheng, D.C. Zhang, H.X. Ju, S.J. Ding, Electrochemical aptasensor based on klenow fragment polymerase reaction for ultrasensitive detection of PDGF-BB, Int. J. Electrochem. Sci. 7 (2012) 8533–8542.
[152] D.L. Liao, H.P. Jiao, B. Wang, Q. Lin, C. Yu, KF polymerase-based fluorescence aptasensor for the label-free adenosine detection, Analyst 137 (2012) 978–982.

[153] Y.B. Li, R.M. Li, L. Zhou, M.J. Zhang, L.S. Ling, Fluorometric determination of Simian virus 40 based on strand displacement amplification and triplex DNA using a molecular beacon probe with a guanine-rich fragment of the stem region, Microchim. Acta 184 (2017) 557–562.
[154] H. Xu, B.T. Wu, J. Wang, H.W. Cao, J. Yang, K.X. Hao, S. Chen, S. Ye, Z.F. Shen, Label-free detection of cancer related gene based on target recycling and palindrome-mediated strand displacement amplification, Talanta 215 (2020), 120897.
[155] Y. Ning, J. Hu, K. Wei, G.L. He, T. Wu, F.G. Lu, Fluorometric determination of mercury(II) via a graphene oxide-based assay using exonuclease III-assisted signal amplification and thymidine–Hg(II)–thymidine interaction, Microchim. Acta 186 (2019) 216.
[156] T. Bao, H.W. Shu, W. Wen, X.H. Zhang, S.F. Wang, A sensitive electrochemical aptasensor for ATP detection based on exonuclease III-assisted signal amplification strategy, Anal. Chim. Acta 862 (2015) 64–69.
[157] K. Zhang, T.L. Ren, K. Wang, X. Zhu, H. Wu, M.H. Xie, Sensitive and selective amplified visual detection of cytokines based on exonuclease III-aided target recycling, Chem. Commun. 50 (2014) 13342–13345.
[158] H. Shi, T. Jin, J.W. Zhang, X.T. Huang, C.Y. Tan, Y.Y. Yang, Y. Tan, A novel aptasensor strategy for protein detection based on G-quadruplex and exonuclease III-aided recycling amplification, Chin. Chem. Lett. 31 (2020) 155–158.
[159] C.F. Chen, J.J. Zhao, J.H. Jiang, R.Q. Yu, A novel exonuclease III-aided amplification assay for lysozyme based on graphene oxide platform, Talanta 101 (2012) 357–361.
[160] H. Wu, R.J. Liu, X.J. Kang, C.Y. Liang, L. Lv, Z.J. Guo, Fluorometric aptamer assay for ochratoxin A based on the use of single walled carbon nanohorns and exonuclease III-aided amplification, Microchim. Acta 185 (2018) 27.
[161] W.H. Bai, C. Zhu, J.C. Liu, M.M. Yan, S.M. Yang, A.L. Chen, Split aptamer-based sandwich fluorescence resonance energy transfer assay for 19-nortestosterone, Microchim. Acta 183 (2016) 2533–2538.
[162] C.Y. Zhou, Z. Yu, W.L. Yu, H.W. Liu, H. Zhang, C.L. Guo, Split aptamer-based detection of adenosine triphosphate using surface enhanced Raman spectroscopy and two kinds of gold nanoparticles, Microchim. Acta 186 (2019) 251.
[163] M.F. Fatin, A.R. Ruslinda, S.C.B. Gopinath, M.K.M. Arshad, U. Hashim, T. Lakshmipriya, T.H. Tang, A. Kamarulzaman, Co-ordinated split aptamer assembly and disassembly on Gold nanoparticle for functional detection of HIV-1 tat, Process Biochem. 79 (2019) 32–39.
[164] F.D. Morris, E.M. Peterson, J.M. Heemstra, J.M. Harris, Single-molecule kinetic investigation of cocaine-dependent split-aptamer assembly, Anal. Chem. 90 (2018) 12964–12970.
[165] B.Y. Yuan, L.Y. Guo, K. Yin, X.Y. Wang, Q. Liu, M.M. He, K.D. Liu, J.M. Zhao, Highly sensitive and specific detection of tumor cells based on a split aptamer-triggered dual hybridization chain reaction, Analyst 145 (2020) 2676–2681.
[166] G.Z. Zhu, G. Niu, X.Y. Chen, Aptamer–drug conjugates, Bioconjug. Chem. 26 (2015) 2186–2197.
[167] M. Rimmele, Nucleic acid aptamers as tools and drugs: recent developments, ChemBioChem 4 (2003) 963–971.
[168] A.C. Yan, M. Levy, Aptamers and aptamer targeted delivery, RNA Biol. 6 (2009) 316–320.
[169] P. Röthlisberger, C. Gasse, M. Hollenstein, Nucleic acid aptamers: emerging applications in medical imaging, nanotechnology, neurosciences, and drug delivery, Int. J. Mol. Sci. 18 (2017) 2430.
[170] T.K. Wood, B.A.F. González, M. Herzberg, J. Lee, Motility influences biofilm architecture in *Escherichia coli*, Appl. Microbiol. Biotechnol. 72 (2006) 361–367.
[171] Y. Ning, L.J. Cheng, M. Ling, X.R. Feng, L.L. Chen, M.X. Wu, L. Deng, Efficient suppression of biofilm formation by a nucleic acid aptamer, Pathog. Dis. 73 (2015) ftv034.
[172] J.J. Skehel, D.C. Wiley, Receptor binding and membrane fusion in virus entry: the influenza hemagglutinin, Annu. Rev. Biochem. 69 (2000) 531–569.
[173] W.K. Li, X.R. Feng, X. Yan, K.Y. Liu, L. Deng, A DNA aptamer against influenza a virus: an effective inhibitor to the hemagglutinin-glycan interactions, Nucleic Acid Ther. 26 (2016) 166–172.
[174] J.R. Wyatt, T.A. Vickers, J.L. Roberson, R.W. Buckheit Jr, T. Klimkait, E. DeBaets, P.W. Davis, B. Rayner, J.L. Imbach, D.J. Ecker, Combinatorially selected guanosine-quartet structure is a potent inhibitor of human immunodeficiency virus envelope-mediated cell fusion, Proc. Natl. Acad. Sci. U. S. A. 91 (1994) 1356–1360.
[175] J.H. Zhou, P. Swiderski, H.T. Li, J. Zhang, C.P. Neff, R. Akkina, J.J. Rossi, Selection, characterization and application of new RNA HIV gp 120 aptamers for facile delivery of Dicer substrate siRNAs into HIV infected cells, Nucleic Acids Res. 37 (2009) 3094–3109.
[176] J.J. DeStefano, G.R. Nair, Novel aptamer inhibitors of human immunodeficiency virus reverse transcriptase, Oligonucleotides 18 (2008) 133–144.
[177] L. Krishnan, A. Engelman, Retroviral integrase proteins and HIV-1 DNA integration, J. Biol. Chem. 287 (2012) 40858–40866.
[178] S. Duclair, A. Gautam, A. Ellington, V.R. Prasad, High-affinity RNA aptamers against the HIV-1 protease inhibit both in vitro protease activity and late events of viral replication, Mol. Ther. Nucleic Acids 4 (2015) e228.
[179] D. Ramalingam, S. Duclair, S.A. Datta, A. Ellington, A. Rein, V.R. Prasad, RNA aptamers directed to human immunodeficiency virus type 1 Gag polyprotein bind to the matrix and nucleocapsid domains and inhibit virus production, J. Virol. 85 (2011) 305–314.
[180] K.J. Jang, N.R. Lee, W.S. Yeo, Y.J. Jeong, D.E. Kim, Isolation of inhibitory RNA aptamers against severe acute respiratory syndrome (SARS) coronavirus ntpase/helicase, Biochem. Biophys. Res. Commun. 366 (2008) 738–744.
[181] C. Nicol, O. Cesur, S. Forrest, T.A. Belyaeva, D.H. Bunka, G.E. Blair, N. J. Stonehouse, An RNA aptamer provides a novel approach for the induction of apoptosis by targeting the HPV16 E7 oncoprotein, PLoS One 8 (2013), e64781.
[182] S. Muller, P. Moller, M.J. Bick, S. Wurr, S. Becker, S. Gunther, B.M. Kummerer, Inhibition of filovirus replication by the zinc finger antiviral protein, J. Virol. 81 (2007) 2391–2400.
[183] C.R. Ireson, L.R. Kelland, Discovery and development of anticancer aptamers, Mol. Canc. Therapeut. 5 (2006) 2957–2962.
[184] S. Soundararajan, L. Wang, V. Sridharan, W. Chen, N. Courtenay-Luck, D. Jones, E.K. Spicer, D.J. Fernandes, Plasma membrane nucleolin is a receptor for the anticancer aptamer as1411 in mv4-11 leukemia cells, Mol. Pharmacol. 76 (2009) 984–991.
[185] F. Mongelard, P. Bouvet, AS-1411, a guanosine-rich oligonucleotide aptamer targeting nucleolin for the potential treatment of cancer, including acute myeloid leukemia, Curr. Opin. Mol. Ther. 12 (2010) 107–114.
[186] S. Soundararajan, W.W. Chen, E.K. Spicer, N. Courtenay-Luck, D.J. Fernandes, The nucleolin targeting aptamer as1411 destabilizes bcl-2 messenger rna in human breast cancer cells, Cancer Res. 68 (2008) 2358–2365.
[187] A.C. Girvan, Y. Teng, L.K. Casson, S.D. Thomas, S. Jüliger, M.W. Ball, J.B. Klein, W.M. Pierce Jr, S.S. Barve, P.J. Bates, AGRO100 inhibits activation of nuclear factor-kappaB (NF-kappaB) by forming a complex with NF-kappaB essential modulator (NEMO) and nucleolin, Mol. Cancer Ther. 5 (2006) 1790–1799.
[188] R.E. Carter, A.R. Feldman, J.T. Coyle, Prostate-specific membrane antigen is a hydrolase with substrate and pharmacologic characteristics of a neuropeptidase, Proc. Natl. Acad. Sci. U. S. A. 93 (1996) 749–753.
[189] J.P. Dassie, L.I. Hernandez, G.S. Thomas, M.E. Long, W.M. Rockey, C.A. Howell, Y.N. Chen, F.J. Hernandez, X.Y. Liu, M.E. Wilson, L.A. Allen, D.A. Vaena, D. K. Meyerholz, P.H. Giangrande, Targeted inhibition of prostate cancer metastases with an RNA aptamer to prostate-specific membrane antigen, Mol. Ther. 22 (2014) 1910–1922.
[190] G. Mahlknecht, R. Maron, M. Mancini, B. Schechter, M. Sela, Y. Yarden, Aptamer to ErbB-2/HER2 enhances degradation of the target and inhibits tumorigenic growth, Proc. Natl. Acad. Sci. U. S. A. 110 (2013) 8170–8175.
[191] B. Sennino, B.L. Falcon, D. McCauley, T. Le, T. McCauley, J.C. Kurz, A. Haskell, D. M. Epstein, D.M. McDonald, Sequential loss of tumor vessel pericytes and endothelial cells after inhibition of platelet-derived growth factor B by selective aptamer AX102, Cancer Res. 67 (2007) 7358–7367.
[192] R. Fontanella, S. Camorani, L. Cerchia, A. Zannetti, PDGFR? Inhibition by Gint4.T aptamer prevents recruitment of bone marrow-derived mesenchymal stem cells into breast cancer microenvironment, Eur. J. Cancer 61 (2016) S55.
[193] D. Zboralski, K. Hoehlig, D. Eulberg, A. Vater, A. Frömming, Increasing tumor-infiltrating t cells through inhibition of CXCL12 with NOX-A12 synergizes with PD-1 blockade, Cancer Immunol. Res. 5 (2017) 950–956.
[194] J.O. McNamara II, D. Kolonias, F. Pastor, R.S. Mittler, L.P. Chen, P.H. Giangrande, B. Sullenger, E. Gilboa, Multivalent 4-1BB binding aptamers costimulate CD8 + T cells and inhibit tumor growth in mice, J. Clin. Invest. 118 (2008) 377–386.
[195] A.A. Moshfeghi, C.A. Puliafito, Pegaptanib sodium for the treatment of neovascular age-related macular degeneration, Expert. Opin. Inv. Drug. 14 (2005) 671–682.
[196] T. Ganz, Hepcidin, a key regulator of iron metabolism and mediator of anemia of inflammation, Blood 102 (2003) 783–788.
[197] J.L. Diener, H.A.D. Lagasse, D. Duerschmied, Y. Merhi, J.F. Tanguay, R. Hutabarat, J. Gilbert, D.D. Wagner, R. Schaub, Inhibition of von Willebrand factor-mediated platelet activation and thrombosis by the anti-von Willebrand factor A1-domain aptamer ARC1779, J. Thromb. Haemost. 7 (2009) 1155–1162.
[198] Y.Q. Li, H.B. You, Self-assembled polyethylenimine-graft-poly(ε-caprolactone) micelles as potential dual carriers of genes and anticancer drugs, Biomaterials 28 (2007) 4132–4142.
[199] K. Kawakami, H. Nishida, N. Tatewaki, Y. Nakajima, T. Konishi, M. Hirayama, Persimmon leaf extract inhibits the atm activity during dna damage response induced by doxorubicin in a549 lung adenocarcinoma cells, Biosci. Biotech. Bioch. 75 (2011) 650–655.
[200] S.B. Mei, L. Hong, X.Y. Cai, B. Xiao, P. Zhang, L. Shao, Oxidative stress injury in doxorubicin-induced cardiotoxicity, Toxicol. Lett. 307 (2019) 41–48.
[201] V. Bagalkot, O.C. Farokhzad, R. Langer, S.Y. Jon, An aptamer-doxorubicin physical conjugate as a novel targeted drug-delivery platform, Angew. Chem. Int. Ed. 45 (2006) 8149–8152.
[202] J. Macdonald, D. Denoyer, J. Henri, A. Jamieson, I.J.G. Burvenich, N. Pouliot, S. Shigdar, Bifunctional aptamer-doxorubicin conjugate crosses the blood-brain barrier and selectively delivers its payload to EpCAM-positive tumor cells, Nucleic Acid Ther. 30 (2020) 117–128.
[203] Y.F. Huang, D.H. Shangguan, H.P. Liu, J.A. Phillips, X.L. Zhang, Y. Chen, W. H. Tan, Molecular assembly of an aptamer-drug conjugate for targeted drug delivery to tumor cells, Chembiochem 10 (2009) 862–868.
[204] R.W. Wang, G. Zhu, L. Mei, Y. Xie, H. Ma, M. Ye, F.L. Qing, W.H. Tan, Automated modular synthesis of aptamer-drug conjugates for targeted drug delivery, J. Am. Chem. Soc. 136 (2014) 2731–2734.
[205] B.K. Yoo, P.K. Santhekadur, R. Gredler, D. Chen, L. Emdad, S. Bhutia, L. Pannell, P.B. Fisher, D. Sarkar, Increased RNA-induced silencing complex (RISC) activity contributes to hepatocellular carcinoma, Hepatology 53 (2011) 1528–1548.
[206] A.D. Redfern, S.M. Colley, D.J. Beveridge, N. Ikeda, P.J. Leedman, Rna-induced silencing complex (risc) proteins pact, trbp, and dicer are sra binding nuclear receptor coregulators, Proc. Natl. Acad. Sci. U. S. A. 110 (2013) 6536–6541.
[207] J.O. McNamara II, E.R. Andrechek, Y. Wang, K.D. Viles, R.E. Rempel, E. Gilboa, B. A. Sullenger, P.H. Giangrande, Cell type-specific delivery of siRNAs with aptamer-siRNA chimeras, Nat. Biotechnol. 24 (2006) 1005–1015.

[208] H.Y. Liu, X.L. Yu, H.T. Liu, D.Q. Wu, J.X. She, Co-targeting EGFR and survivin with a bivalent aptamer-dual siRNA chimera effectively suppresses prostate cancer, Sci. Rep. 6 (2016) 30346.
[209] M. Kortylewski, P. Swiderski, A. Herrmann, L. Wang, C. Kowolik, M. Kujawski, H. Lee, A. Scuto, Y. Liu, C.M. Yang, J.H. Deng, H.S. Soifer, A. Raubitschek, S. Forman, J.J. Rossi, D.M. Pardoll, R. Jove, H. Yu, In vivo delivery of sirNA to immune cells by conjugation to a tlr9 agonist enhances antitumor immune responses, Nat. Biotechnol. 27 (2009) 925–932.
[210] J.H. Zhou, K. Tiemann, P. Chomchan, J. Alluin, P. Swiderski, J. Burnett, X. Z. Zhang, S. Forman, R. Chen, J. Rossi, Dual functional BAFF receptor aptamers inhibit ligand-induced proliferation and deliver siRNAs to NHL cells, Nucleic Acids Res. 41 (2013) 4266–4283.
[211] J.H. Zhou, H.T. Li, S. Li, J. Zaia, J. Rossi, Novel dual inhibitory function aptamer-siRNA delivery system for HIV-1 therapy, Mol. Ther. 16 (2008) 1481–1489.
[212] J.H. Zhou, J. Rossi, Therapeutic potential of aptamer-siRNA conjugates for treatment of HIV-1, BioDrugs 26 (2012) 393–400.
[213] C.T. Matea, T. Mocan, F. Tabaran, T. Pop, O. Mosteanu, C. Puia, C. Iancu, L. Mocan, Quantum dots in imaging, drug delivery and sensor applications, Int. J. Nanomed. Nanosurg. 12 (2017) 5421–5431.
[214] N. Bajwa, N.K. Mehra, K. Jain, N.K. Jain, Pharmaceutical and biomedical applications of quantum dots, Artif. Cell. Nanomed. B 44 (2016) 758–768.
[215] V. Bagalkot, L.F. Zhang, E. Levy-Nissenbaum, S. Jon, P.W. Kantoff, R. Langer, O. C. Farokhzad, Quantum dot-aptamer conjugates for synchronous cancer imaging, therapy, and sensing of drug delivery based on Bi-fluorescence resonance energy transfer, Nano Lett. 7 (2007) 3065–3070.
[216] R. Savla, O. Taratula, O. Garbuzenko, T. Minko, Tumor targeted quantum dot-mucin 1 aptamer-doxorubicin conjugate for imaging and treatment of cancer, J. Control. Release 153 (2011) 16–22.
[217] H. Sun, F. Zhang, H. Wei, B. Yang, The effects of composition and surface chemistry on the toxicity of quantum dots, J. Mater. Chem. B 1 (2013) 6485–6494.
[218] A. Hoshino, S. Hanada, K. Yamamoto, Toxicity of nanocrystal quantum dots: the relevance of surface modifications, Arch. Toxicol. 85 (2011), 721-721.
[219] J. Zhang, L. Mou, X. Jiang, Surface chemistry of gold nanoparticles for health-related applications, Chem. Sci. 11 (2020) (2020) 923–936.
[220] A.A. Aldhabi, Characterization of gold nanoparticles and study influence on physical properties of pva/pvp nanocomposites, Int. J. Biol. Macromol. 86 (2020) 789–798.
[221] Y.L. Luo, Y.S. Shiao, Y.F. Huang, Release of photoactivatable drugs from plasmonic nanoparticles for targeted cancer therapy, ACS Nano 5 (2011) 7796–7804.
[222] A. Latorre, C. Posch, Y. Garcimartín, A. Celli, M. Sanlorenzo, L. Vujic, M. Ma, M. Zekhtser, K. Rappersberger, S. Ortiz-Urda, Á. Somoza, DNA and aptamer stabilized gold nanoparticles for targeted delivery of anticancer therapeutics, Nanoscale 6 (2014) 7436–7442.
[223] Y.S. Shiao, H.H. Chiu, P.H. Wu, Y.F. Huang, Aptamer-functionalized gold nanoparticles as photoresponsive nanoplatform for Co-drug delivery, ACS Appl. Mater. Interfaces 6 (2014) 21832–21841.
[224] S.Y. Zhu, G.B. Xu, Single-walled carbon nanohorns and their applications, Nanoscale 2 (2010) 2538–2549.
[225] Y. Wang, Z.H. Li, J. Wang, J.H. Li, Y.H. Lin, Graphene and graphene oxide: biofunctionalization and applications in biotechnology, Cell 29 (2012) 205–212.
[226] H.J. Zhang, L. Hou, X.J. Jiao, Y.D. Ji, X.L. Zhu, H.J. Li, X.Z. Chen, J.X. Ren, Y. D. Xia, Z.Z. Zhang, In vitro and in vivo evaluation of antitumor drug-loaded aptamer targeted single-walled carbon nanotubes system, Curr. Pharm. Biotechnol. 14 (2014) 1105–1117.
[227] S. Taghavi, A.H. Nia, K. Abnous, M. Ramezani, Polyethylenimine-functionalized carbon nanotubes tagged with as1411 aptamer for combination gene and drug delivery into human gastric cancer cells, Int. J. Pharmaceut. 516 (2017) 301–312.
[228] Y.M. Yu, P. Wu, Y.J. Yin, H. Zhang, C.X. Cai, Aptamer-functionalized graphene oxide for highly efficient loading and cancer cell-specific delivery of antitumor drug, J. Mater. Chem. B 2 (2014) 3849–3859.
[229] M. Alibolandi, M. Mohammadi, S.M. Taghdisi, M. Ramezani, K. Abnous, Fabrication of aptamer decorated dextran coated nano-graphene oxide for targeted drug delivery, Carbohydr. Polym. 155 (2017) 218–229.
[230] Y.X. Tang, H. Hu, M.G. Zhang, J.B. Song, L.M. Nie, S.J. Wang, G. Niu, P. Huang, G. M. Lu, X.Y. Chen, Aptamer-targeting photoresponsive drug delivery system using "off-on" graphene oxide wrapped mesoporous silica nanoparticles, Nanoscale 7 (2015) 6304–6310.
[231] X.Y. Zhang, W.B. Hu, J. Li, L. Tao, Y. Wei, A comparative study of cellular uptake and cytotoxicity of multi-walled carbon nanotubes, graphene oxide, and nanodiamond, Toxicol. Res. 1 (2012) 62–68.
[232] X.T. Liu, X.Y. Mu, X.L. Wu, L.X. Meng, W.B. Guan, Y.Q. Ma, H. Sun, C.J. Wang, X. F. Li, Toxicity of multi-walled carbon nanotubes, graphene oxide,and reduced graphene oxide to zebrafish embryos, Biomed. Environ. Sci. 27 (2014) 676–683.
[233] R.F. Hamilton, Z.Q. Wu, M. Thakkar, A. Holian, S. Mitra, Modification of nano-silver bioactivity by adsorption on carbon nanotubes and graphene oxide, Inhal. Toxicol. 30 (2018) 429–438.
[234] X. Hu, Z. Wei, L. Mu, Graphene oxide nanosheets at trace concentrations elicit neurotoxicity in the offspring of zebrafish, Carbon 117 (2017) 182–191.
[235] L. Huang, A.L. Klibanov, A. Mori, X. Cao, Targeted delivery of drugs and DNA with liposomes, J. Liposome Res. 3 (1993) 505–515.
[236] Z. Zhao, C. Chen, C. Xie, Y. Zhao, Design, synthesis and evaluation of liposomes modified with dendritic aspartic acid for bone-specific targeting, Chem. Phys. Lipids 226 (2019), 104832.
[237] H. Xing, L. Tang, X.J. Yang, K. Hwang, W.D. Wang, Q. Yin, N.Y. Wong, L. W. Dobrucki, N. Yasui, J.A. Katzenellenbogen, W.G. Helferich, J.J. Cheng, Y. Lu, Selective delivery of an anticancer drug with aptamer-functionalized liposomes to breast cancer cells in vitro and in vivo, J. Mater. Chem. B 1 (2013) 5288–5297.
[238] D.M. Kim, M. Kim, H.B. Park, K.S. Kim, D.E. Kim, Anti-MUC1/CD44 dual-aptamer-conjugated liposomes for cotargeting breast cancer cells and cancer stem cells, ACS Appl. Biol. Mater. 2 (2019) 4622–4633.
[239] M.W. Kim, H.Y. Jeong, S.J. Kang, I.H. Jeong, M.J. Choi, Y.M. You, C.S. Im, I. H. Song, T.S. Lee, J.S. Lee, A. Lee, Y.S. Park, Anti-EGF receptor aptamer-guided co-delivery of anti-cancer siRNAs and quantum dots for theranostics of triple-negative breast cancer, Theranostics 9 (2019) 837–852.
[240] S. Yu, X.J. Bi, S.G. Wu, Y.T. Yu, B.J. Jiang, A.W. Zhang, K. Lan, S.L. Duan, Co-delivery of paclitaxel and PLK1-targeted siRNA using aptamer-functionalized cationic liposome for synergistic anti-breast cancer effects in vivo, J. Biomed. Nanotechnol. 15 (2019) 1135–1148.
[241] N. Grimaldi, F. Andrade, N. Segovia, L. Ferrer-Tasies, S. Sala, J. Veciana, N. Ventosa, Lipid-based nanovesicles for nanomedicine, Chem. Soc. Rev. 45 (2016) 6520–6545.
[242] A.A. Khan, K.S. Allemailem, S.A. Almatroodi, A. Almatroudi, A.H. Rahmani, Recent strategies towards the surface modification of liposomes: an innovative approach for different clinical applications, 3 Biotech 10 (2020) 1–15.